Reprinted from
ICARUS 101, 108–128 (1993)

Habitable Zones around Main Sequence Stars

JAMES F. KASTING

Department of Geosciences, 211 Deike, Penn State University, University Park, Pennsylvania 16802

DANIEL P. WHITMIRE

Department of Physics, University of Southwestern Louisiana, Lafayette, Louisiana 70504-4210

AND

RAY T. REYNOLDS

Space Science Division, MS 245-3, NASA Ames Research Center, Moffett Field, California 94035

Received April 27, 1992; revised October 2, 1992

A one-dimensional climate model is used to estimate the width of the habitable zone (HZ) around our Sun and around other main sequence stars. Our basic premise is that we are dealing with Earth-like planets with $CO_2/H_2O/N_2$ atmospheres and that habitability requires the presence of liquid water on the planet's surface. The inner edge of the HZ is determined in our model by loss of water via photolysis and hydrogen escape. The outer edge of the HZ is determined by the formation of CO_2 clouds, which cool a planet's surface by increasing its albedo and by lowering the convective lapse rate. Conservative estimates for these distances in our own Solar System are 0.95 and 1.37 AU, respectively; the actual width of the present HZ could be much greater. Between these two limits, climate stability is ensured by a feedback mechanism in which atmospheric CO_2 concentrations vary inversely with planetary surface temperature. The width of the HZ is slightly greater for planets that are larger than Earth and for planets which have higher N_2 partial pressures. The HZ evolves outward in time because the Sun increases in luminosity as it ages. A conservative estimate for the width of the 4.6-Gyr continuously habitable zone (CHZ) is 0.95 to 1.15 AU.

Stars later than F0 have main sequence lifetimes exceeding 2 Gyr and, so, are also potential candidates for harboring habitable planets. The HZ around an F star is larger and occurs farther out than for our Sun; the HZ around K and M stars is smaller and occurs farther in. Nevertheless, the widths of all of these HZs are approximately the same if distance is expressed on a logarithmic scale. A log distance scale is probably the appropriate scale for this problem because the planets in our own Solar System are spaced logarithmically and because the distance at which another star would be expected to form planets should be related to the star's mass. The width of the CHZ around other stars depends on the time that a planet is required to remain habitable and on whether a planet that is initially frozen can be thawed by modest increases in stellar luminosity. For a specified period of habitability, CHZs around K and M stars are wider (in log distance) than for our Sun because these stars evolve more slowly. Planets orbiting late K stars and M stars may not be habitable, however, because they can become trapped in synchronous rotation as a consequence of tidal damping. F stars have narrower (log distance) CHZ's than our Sun because they evolve more rapidly. Our results suggest that mid-to-early K stars should be considered along with G stars as optimal candidates in the search for extraterrestrial life.

I. INTRODUCTION

Astronomers have been interested for many years in the possibility of life on other planets in our own Solar System and in other planetary systems. The region around a star in which life-supporting planets can exist has been termed the "habitable zone" (Huang 1959, 1960), or the "ecosphere" (Dole 1964, Shklovski and Sagan 1966). Its limits are defined by assumed climatic constraints which differ from one author to the next. Dole (1964), for example, defined a habitable planet as one on which at least 10% of the surface had a mean temperature of between 0 and 30°C, with extremes not to exceed −10 or 40°C. These limits are appropriate for habitation by humans. Others (e.g., Rasool and DeBergh 1970, Hart 1978, Kasting *et al.* 1988, Whitmire *et al.* 1991) have equated habitability with the presence of liquid water on a planet's surface. The idea here is that all organisms with which we are familiar require liquid water during at least part of their life cycle. Fogg (1992) has considered both definitions, using the term "biocompatible" to describe planets possessing liquid water and reserving the term "habit-

0019-1035/93 $5.00

able" for those planets suitable for humans. We ourselves are more interested in determining if life can evolve on other planets than we are in colonizing them, so we will use the presence of liquid water as our habitability criterion. For ease of presentation, we will refer to the liquid-water region as the habitable zone, or "HZ," recognizing that not all planets in this region would make suitable homes for humans.

The estimated width of the HZ around our Sun has fluctuated substantially over the last 30 years. Despite his relatively restrictive climatic assumptions, Dole (1964) predicted that the HZ should extend from 0.725 AU out to 1.24 AU, that is, from close to the orbit of Venus to about halfway between Earth and Mars. The reason for this optimistic result is that Dole's "Earth-like" planets had optically thin atmospheres and fixed planetary albedos. In reality, Earth's atmosphere is optically thick at most infrared wavelengths; this gives rise to a greenhouse effect of about 33°C. Furthermore, Earth's albedo almost certainly fluctuates in response to changes in the distribution of snow, ice, and clouds. Both the greenhouse effect and the planetary albedo are subject to well understood positive feedbacks: the greenhouse effect increases with surface temperature because of increased atmospheric water vapor (Manabe and Wetherald 1967), while the planetary albedo is enhanced at cold surface temperatures by increased ice and snow cover. These positive feedbacks can have destabilizing effects on planetary climates. Using a one-dimensional, radiative-equilibrium climate model, Rasool and DeBergh (1970) calculated that the oceans would have never condensed had Earth been situated 4 to 7% closer to the Sun. This fate has been termed the "runaway greenhouse." On the other hand, simple energy-balance climate models (Budyko 1969, Sellers 1969, North 1975) predict that the Earth would have become globally glaciated had it formed only 1 to 2% farther from the Sun.

The Sun's HZ is also affected by solar evolution. The Sun, like other stars, increases in luminosity during its lifetime on the main sequence (Newman and Rood 1977, Gough 1981, Gilliland 1989). According to these models, the Sun was approximately 30% dimmer when the Solar System formed, ~4.6 Gyr ago, and will increase to nearly three times its present luminosity by the time it leaves the main sequence, about 5 Gyr hence (Iben 1967a). Hart (1978) was the first to include solar evolution in a model of planetary habitability. He also tried to evolve the planet's atmosphere at the same time—an ambitious undertaking, given the complexity of the problem. Hart concluded that Earth would have experienced a runaway greenhouse at some time during its history had it formed inside 0.95 AU and would have encountered runaway glaciation had it formed outside 1.01 AU. Hart termed the region between these limits the "continuously habitable zone," or "CHZ." In a subsequent paper, Hart (1979) investigated CHZ's around other main sequence stars and concluded that they were generally narrower than the CHZ for our own Sun and disappeared altogether for stars later than K0. Hart's results have been cited by others (e.g., Pollard 1979, Rood and Trefil 1981) as evidence that habitable planets may be very scarce. While we do not agree with Hart's conclusions, for reasons to be described below, we do agree that stellar evolution provides important constraints on planetary habitability.

The paper is organized as follows: Section 2 describes a mechanism for stabilizing climate on the Earth and other Earth-like planets. Section 3 discusses the physical processes that define the inner and outer boundaries of the HZ and points out constraints obtained from Venus and Mars. Sections 4 and 5 describe our one-dimensional climate model and show how it is used to estimate the width of the HZ and the CHZ around our own Sun. This analysis is extended to other main sequence stars in Section 6, wherein we also discuss the questions of whether other stars have planets and where such planets might be located with respect to the HZ. Section 7 summarizes our results and discusses the implications for NASA's SETI (Search for Extraterrestrial Intelligence) project.

2. CLIMATE STABILIZATION BY THE CARBONATE–SILICATE CYCLE

The main reason we do not concur with Hart's pessimistic analysis is that his model neglected a strong negative feedback that should help to stabilize planetary climates, namely, the link between atmospheric CO_2 level and surface temperature first proposed by Walker *et al.* (1981). [There are other problems with Hart's model as well, some of which have been discussed by Schneider and Thompson (1980).] The climate stabilization argument has been made before (e.g., Kasting *et al.* 1988, Kasting and Toon 1989); we reiterate it here because it is essential to our discussion of planetary habitability. On long time scales ($t > 10^6$ years), the CO_2 concentration of Earth's atmosphere is controlled by slow interactions with the crustal rock reservoir, a process referred to as the carbonate–silicate cycle. CO_2 is removed from the atmosphere by the weathering of calcium and magnesium silicates in rocks and the subsequent precipitation and burial of carbonate sediments. If one represents all silicate rocks by the mineral wollastonite ($CaSiO_3$), the initial weathering reaction can be written as

$$CaSiO_3 + 2CO_2 + H_2O \rightarrow Ca^{++} + 2HCO_3^- + SiO_2. \quad (1)$$

The dissolved products of silicate weathering are carried

by streams and rivers down to the ocean where organisms use them to make shells of calcium carbonate,

$$Ca^{++} + 2HCO_3^- \rightarrow CaCO_3 + CO_2 + H_2O. \quad (2)$$

[Although most $CaCO_3$ is precipitated biotically today, the same reaction would occur in the absence of the biota, albeit at a higher bicarbonate concentration. Life is not, therefore, required to complete this part of the carbonate–silicate cycle (Walker 1991).] When the organisms die these shells fall to the seafloor. Most dissolve on the way down, but a fraction, specifically those buried at relatively shallow depths, survive and become incorporated in carbonate sediments. The overall reaction, adding reactions (1) and (2), is

$$CaSiO_3 + CO_2 \rightarrow CaCO_3 + SiO_2. \quad (3)$$

Reaction (3) is similar in form to the equilibrium reaction that was thought by Urey (1952) to control the CO_2 content of the atmosphere; here, however, it represents part of a nonequilibrium geochemical cycle.

Although weathering reactions are slow, the estimated rate of silicate weathering is sufficient to remove all the carbon in the combined atmosphere/ocean system in about 400 million years (Myr) (Holland 1978, Berner *et al.* 1983). Thus, some process must restore carbon to the system in order to maintain a steady state. The process that returns CO_2 is carbonate metamorphism, which occurs when the seafloor is subducted and carbonate sediments are exposed to high temperatures and pressures. Under these conditions, reaction (3) reverses direction: calcium silicate is reformed and gaseous CO_2 is released and vented back to the atmosphere by volcanos.

The negative feedback important to the climate system resides in reaction (1). Weathering reactions proceed at appreciable rates only in the presence of liquid water. If Earth ever became cold enough so that the oceans froze, silicate weathering would virtually cease and CO_2 would begin to accumulate in the atmosphere. Within a relatively short time span, geologically speaking, a dense CO_2 atmosphere would be formed and the accompanying greenhouse effect would melt the ice. In a more realistic model, the atmospheric CO_2 level would begin to increase before the oceans actually froze, so that runaway glaciation would probably never occur. [There remains some possibility that a transient runaway glaciation could occur, since the time required to freeze the oceans is much shorter than the time required to build up a dense CO_2 atmosphere (Caldeira and Kasting 1992). This situation can be avoided, however, if the Earth starts out warm.] This feedback mechanism can explain the apparent stability of Earth's climate with respect to the faint young Sun (Walker *et al.* 1981, Kasting 1989), although some authors argue that it would have been much less effective without active participation by the biota (Lovelock and Whitfield 1982, Schwartzman and Volk 1989). We return to this question in Section 5(iii). The same feedback has been postulated as the reason for the apparent warm climate on early Mars (Pollack *et al.* 1987). Based on this argument, Kasting and Toon (1989) suggested that the outer edge of the CHZ in our own Solar System lies beyond the orbit of Mars and that it is ultimately limited by the difficulty of forming a planet too close to the gravitational influence of Jupiter.

The implications of this theory for the existence of habitable planets are just the opposite of Hart's model: provided that other stars have planetary systems, the chances of at least one planet being located within a star's CHZ are fairly good. Fogg (1992) has pursued this idea quantitatively with a computer model that incorporates both stellar evolution and an algorithm for predicting planetary spacing (Dole 1970). (Dole's algorithm has a relatively weak scientific basis; however, it does yield planetary systems that resemble our own.) Assuming an inner edge of 0.95 AU and an outer edge of 2.0 AU for our own Sun's present HZ, he estimates that 1 out of every 39 stars possesses a biocompatible (i.e., liquid water) planet and that 1 out of 413 stars possesses a planet suitable for habitation by humans. If true, the nearest biocompatible and human-habitable planets should lie within 14 and 31 light years, respectively. The prospects for finding life around other stars would thus appear to be very good.

3. CLIMATIC CONSTRAINTS ON THE INNER AND OUTER EDGES OF THE HABITABLE ZONE

Our own thinking on this subject stood at about this point when one of us pointed out that the CO_2/climate buffer would break down if a planet became cold enough for CO_2 to condense (Whitmire *et al.* 1991). Subsequent calculations showed that CO_2 condensation was a serious constraint; indeed, it now appears to preclude a warm, CO_2/H_2O greenhouse on early Mars (Kasting 1991). The reason is twofold: (i) CO_2 condensation produces CO_2 clouds, which should increase a planet's albedo by reflecting incident solar radiation. And, (ii) the latent heat released by condensing CO_2 should reduce the lapse rate in the convective region of a planet's atmosphere, thereby reducing the magnitude of the greenhouse effect. The first effect is difficult to quantify, in part because cloud cover and cloud properties are intrinsically hard to predict and in part because the effect of CO_2 clouds on outgoing infrared radiation can only be calculated with a model that includes scattering at these wavelengths. Our one-dimensional, radiative–convective climate model, like most of its terrestrial counterparts, ignores scattering in the infrared. The

second effect can be readily quantified if one assumes that the convective lapse rate follows a moist CO_2 adiabat in the region where CO_2 is condensing. The actual convective lapse rate can be shallower than the moist adiabat in regions, like terrestrial midlatitudes, where breaking baroclinic waves release significant amounts of energy; however, it should not appreciably exceed the moist adiabat. Using the moist adiabatic lapse rate in a radiative–convective climate model produces the steepest possible lapse rate and, hence, the maximum greenhouse effect for a given set of conditions.

With these thoughts in mind we can use our climate model and our knowledge of Solar System history to identify three possible limits to the outer edge of the HZ around our Sun. The first (and most conservative) limit is the distance at which CO_2 clouds first begin to form in our model, given a fixed surface temperature of 273 K. We term this the "1st condensation" limit. Although we suspect that the HZ extends further than this, we cannot argue this point too strongly because we cannot currently calculate the radiative effect of CO_2 clouds. The second limit, which we term the "maximum greenhouse" limit, is the maximum distance at which a cloud-free, CO_2 atmosphere can maintain a surface temperature of 273 K. This distance can be predicted by our climate model. A third limit, which turns out to be the most optimistic, is based on the hypothesis that early Mars was warm enough to have standing bodies of liquid water. [This inference is disputed by some; see discussion in Kasting (1991).] If one assumes that the valley networks are 3.8 Gyr old (Pollack *et al.* 1987) and that solar luminosity was 75% of its present value at that time (Gough 1981), the effective solar luminosity, S_{eff}, for early Mars was ~32% of the present value at Earth's orbit. The corresponding limit on the outer edge of the HZ today is 1 AU/$S_{\text{eff}}^{0.5}$, or 1.77 AU. This is more distant than the orbit of Mars, 1.52 AU, because the climatic constraint is imposed early in Solar System history. Since this distance exceeds the maximum greenhouse limit for a CO_2–H_2O atmosphere, keeping Mars (or any other planet) warm at this distance may require the presence of additional greenhouse gases (Kasting 1991).

The inner edge of the HZ for our Solar System can be estimated from climate modeling similar to that performed by Kasting (1988). In this model, which will be described below, the mean surface temperature of the "Earth" was raised incrementally from its present value of 288 K up to temperatures exceeding the critical temperature for water (647 K). A moist H_2O adiabat was assumed in the convective region and effective solar luminosity was calculated as a function of surface temperature. Two critical values of S_{eff} were identified: one ($S_{\text{eff}} \sim 1.1$) at which the stratosphere becomes wet and a second ($S_{\text{eff}} \sim 1.4$) at which the oceans evaporate entirely. The first limit is the one which is most relevant to the habitability problem. Once the stratosphere becomes wet, the diffusion restriction on the upward flow of hydrogen is overcome (Hunten 1973, Walker 1977) and hydrogen produced by water vapor photolysis can escape rapidly to space (Kasting and Pollack 1983). Both of the calculated limits ignore the radiative effect of H_2O clouds and are therefore conservative. H_2O clouds in a warm, "moist greenhouse" atmosphere should tend to reduce the surface temperature because their effect on the planetary albedo outweighs their effect on outgoing infrared radiation (Kasting 1988, Fig. 8). Indeed, Ramanathan and Collins (1991) have suggested that cloud negative feedback is so strong that a runaway greenhouse is virtually impossible. We disagree with their conclusion because it implies that Venus must have formed dry, whereas current Solar System formation models (Wetherill 1986) and the high D/H ratio in Venus's atmosphere (Donahue *et al.* 1982, Donahue and Hodges 1992) both suggest that Venus formed wet. [An alternative explanation for the high D/H ratio, based on resupply of atmospheric water by comets, has been proposed by Grinspoon (1987) and Grinspoon and Lewis (1988).] The wet origin model is supported by a recent upward revision of the fractionation factor for deuterium escape (Gurwell and Yung 1992), which makes the cometary resupply model practically untenable.

If we assume that Venus formed wet, we can use the observed absence of water there today to derive a third estimate for the inner edge of the HZ. Radar observations from the Magellan spacecraft and from groundbased telescopes imply that no liquid water has flowed on the Venusian surface for ~1 Gyr (Solomon and Head 1991). The solar flux at Venus' orbit (0.72 AU) 1 Gyr ago was about 1.76 S_0 (Gough 1981). This corresponds to a current HZ inner edge of 0.75 AU. Again, this distance is greater than the orbital distance of Venus because the constraint is imposed at an earlier time in the planet's history. Note that this limit is different from our empirical limit on the outer edge, since Venus is evidently outside of the HZ whereas early Mars was apparently within it.

We thus can derive three different estimates, two completely theoretical and one partly observational, for both the inner and outer edges of the HZ in our own Solar System. The next section describes the climate models used to obtain the theoretical estimates.

4. CLIMATE MODEL DESCRIPTION

The two climate models used in this calculation have been described in detail previously so the presentation here is limited to the essentials. The inner edge calculations were performed with a one-dimensional, radiative–convective climate model similar to that of Kasting (1988), which was itself derived from Kasting *et al.* (1984)

and Kasting and Ackerman (1986). Solar energy deposition was calculated using a δ two-stream scattering routine; infrared absorption was calculated using band models. The infrared calculation was extended down to short wavelengths (0.39 μm) to permit accurate modeling of very hot atmospheres. Nonideal behavior of water vapor was included to ensure accuracy at high surface pressures. Clouds were not included explicitly in the model, but their effect was parameterized by assuming a high surface albedo, $A_s = 0.22$. This value of A_s allows the model to reproduce the Earth's present mean surface temperature, 288 K, given the present solar insolation. Holding A_s constant throughout the calculations is equivalent to assuming zero cloud feedback, which is about the best one can do given our present ignorance of this phenomenon. The model stratosphere was taken to be isothermal at 200 K; this assumption has negligible effect on the runaway greenhouse limit (Kasting 1988, Fig. 3) but may have a significant effect on the "water loss" limit [see Section 5(iv)]. The lapse rate in the model troposphere is moist adiabatic near the top and follows either a dry adiabat or a moist adiabat near the ground, depending on whether the surface temperature is above or below the critical temperature. The lapse rate expressions are given by Eqs. (A4), (A5), (A11), and (A12) in Kasting (1988). Tropospheric relative humidity was assumed to be unity. Both the lapse rate and relative humidity assumptions generate maximum greenhouse warming and, thus, a conservative estimate for the HZ inner edge. An Earth-like planet with a full terrestrial ocean of surface water (1.4×10^{21} liters) is assumed. The background atmosphere consists of 1 bar of N_2 and 300 parts per million by volume (ppmv) of CO_2, with no oxygen or ozone.

The outer edge model is similar to that used by Kasting (1991) to simulate the climate of early Mars, except that it includes N_2 in addition to CO_2. The radiation code is similar to the inner edge model except that the wavelength grid for the infrared was truncated below 0.54 μm. Clouds were neglected and A_s was set equal to 0.215, a value which produces the observed surface temperature for present Mars and which is close to the value needed to simulate a cloud-free Earth. Earth-like planets with 1-bar N_2 atmospheres and variable CO_2 partial pressures were assumed in most of the calculations. Our working hypothesis is that atmospheric CO_2 would accumulate as these planets cooled because of the feedback provided by the carbonate–silicate cycle. Nonideal behavior of CO_2 was included to ensure accuracy at high surface pressures. The calculations were performed for a global mean surface temperature of 273 K using the modeling procedure designated "Method 2" by Kasting (1991). In this method, which is similar to that employed for the inner edge calculations, we specify the surface temperature and then calculate the solar flux required to maintain it. An isothermal stratosphere was assumed; its temperature was calculated by an iterative procedure using the formula

$$T_{\text{strat}} = 167\ \text{K} \left[\frac{S_{\text{eff}}(1 - A_p)}{0.316} \right]^{0.25}. \quad (4)$$

Here, A_p is the planetary albedo and S_{eff} the effective solar flux (in dimensionless units) calculated by the model. This formula successfully reproduces the cold trap temperature at which CO_2 first condenses in a hypothetical, dense Martian atmosphere (Kasting 1991, Fig. 2). The maximum greenhouse limit on the HZ outer edge is relatively insensitive to T_{strat}, as shown below; however, the 1st condensation limit is, not surprisingly, quite dependent on this parameter.

The convective lapse rate in the CO_2-unsaturated part of the troposphere is given by Eq. (A18) in Kasting (1991); the terms C_{pn}, $(\partial V/\partial T)_P$, and $(\partial V/\partial P)_T$ were, however, modified to include a combination of (ideal) N_2 and nonideal CO_2. Specific heats for CO_2 were also modified by using the data of Woolley (1954), cited in Vukalovich and Altunin (1968), to obtain values at zero pressure. [Woolley's values for $C_p(CO_2)$ are 5 to 10% lower than those given by Eq. (A3) of Kasting (1991). This results in a slight increase in predicted lapse rates but not nearly enough to resolve the climate problem for early Mars.] Equation (A18) represents a moist adiabat along which H_2O is condensing. As in the inner edge model, water vapor was assumed to be fully saturated in the troposphere. This has little effect on the outer edge results because most of the greenhouse effect in the cold dense atmospheres studied is attributable to absorption by CO_2. The lapse rate in the CO_2-saturated region was calculated from the expression

$$\frac{d \ln P}{d \ln T} = \frac{d \ln P_v}{d \ln T} - \left(\frac{1}{1 + \alpha_v m_n / \beta m_v} \right) \frac{d \ln \alpha_v}{d \ln T}. \quad (5)$$

Here, P and T are atmospheric pressure and temperature, respectively; P_v is saturation vapor pressure of CO_2; m_n (= 28) and m_v (= 44) are the gram molecular weights of N_2 and CO_2; α_v ($\equiv \rho_v/\rho_n$) is the mass density of CO_2 divided by the density of N_2; and β ($\equiv RT/PV$) is the inverse of the compressibility factor for CO_2. R is the universal gas constant. This expression was derived from Eq. (A5) in Kasting (1988) by manipulating terms. It has the advantage of allowing the first term on the RHS to be calculated directly from the saturation vapor pressure formulas for CO_2 [Eqs. (A5) and (A6) in Kasting 1991]. The second term on the RHS is calculated from Eq. (A4) in Kasting (1988), using CO_2 thermodynamic data from Vukalovich and Altunin (1968). Equation (5) represents

a moist adiabat along which CO_2 condenses. In actuality, H_2O should also condense in this region; however, it is much less abundant than CO_2 so its influence on the lapse rate may be safely neglected.

5. THE HABITABLE ZONE AROUND SOLAR-TYPE STARS

Here, we estimate the width of the HZ and CHZ around stars similar to our own Sun. The first subsection describes the climate modeling results, the next three subsections discuss various uncertainties, and the last subsection factors in time evolution.

(*i*) *Standard Earth Model*

Inner edge. The first set of calculations performed with the model was to estimate the position of the inner and outer edges of the HZ for our standard Earth model. The inner edge computations are shown in Figs. 1–3. These computations are identical to those of Kasting (1988) except for the exclusion of atmospheric O_2. The calculations were performed in the following manner: The surface temperature, T_s, for the model "Earth" was raised incrementally from 220 to 2000 K. At the same time, the radiative model was used to calculate the net incident solar flux, F_S, and the net outgoing infrared flux, F_{IR}, at the top of the atmosphere (Fig. 1a). The solar flux calculation assumes that the flux incident at the top of the atmosphere is equal to the present solar constant at Earth's orbit, $S_0 = 1360$ W m^{-2}. The planetary albedo (Fig. 1b) was then obtained from the expression

$$A_p = 1 - \frac{4F_S}{S_0}. \tag{6}$$

The effective solar flux (Fig. 1c) was found from

$$S_{eff} = \frac{F_{IR}}{F_S}. \tag{7}$$

Recall that S_{eff} ($= S/S_0$) is the normalized solar flux required to maintain a given surface temperature. Equation (7) simply expresses the requirement of planetary energy balance: the net incoming solar radiation must equal the net outgoing infrared.

Physically, the results shown in the figures are explained in the following way: F_{IR} increases with surface temperature to $T_s \simeq 360$ K, then levels off at higher temperatures as the atmosphere becomes optically thick at all infrared wavelengths. Continued increase in F_{IR} occurs only at $T_s > 1400$ K, at which point the surface begins to radiate in the visible. F_S, on the other hand, increases at first because of increased absorption of solar radiation by water vapor, then decreases to a constant value at high

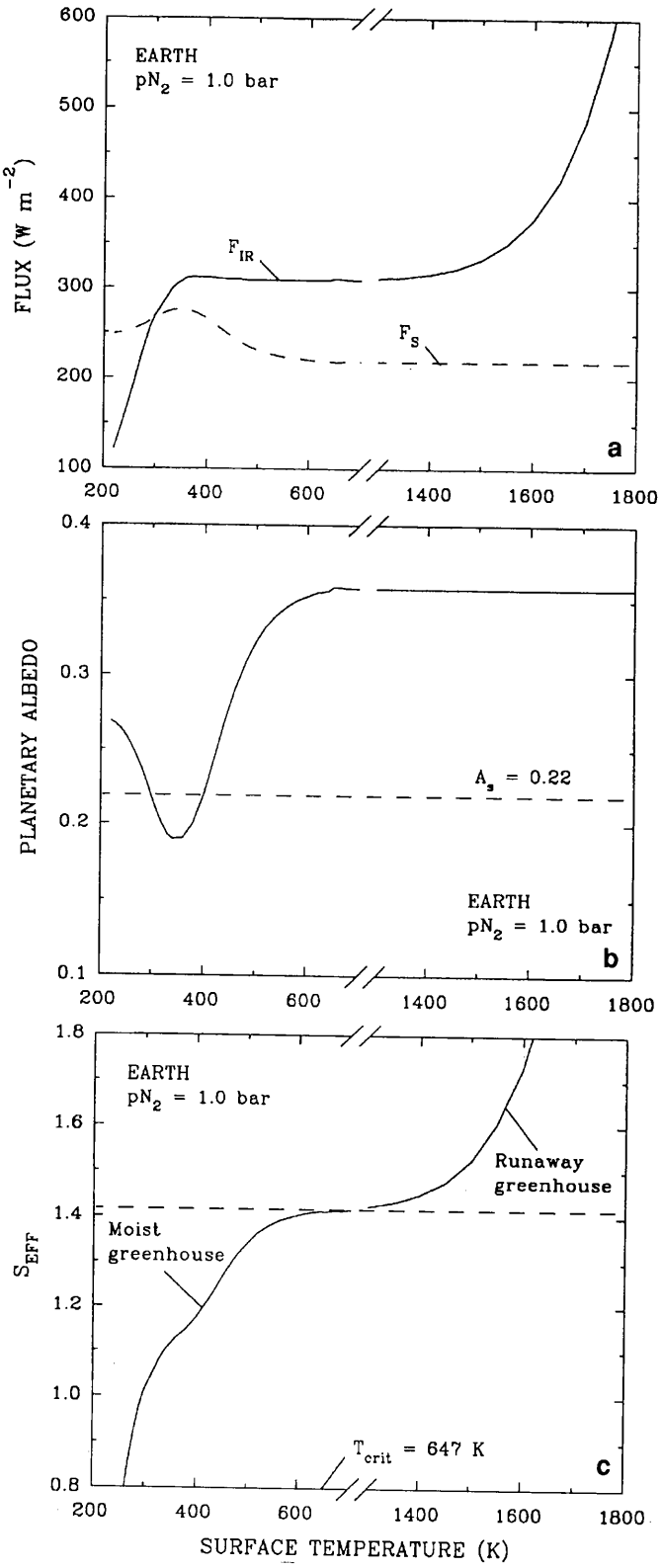

FIG. 1. Dependence of various quantities on surface temperature for the standard inner edge model: (a) outgoing infrared flux (F_{IR}) and net incident solar flux (F_S), (b) planetary albedo, and (c) effective solar flux. Note the scale break between 700 and 1300 K. The dashed curve in (b) shows the assumed surface albedo.

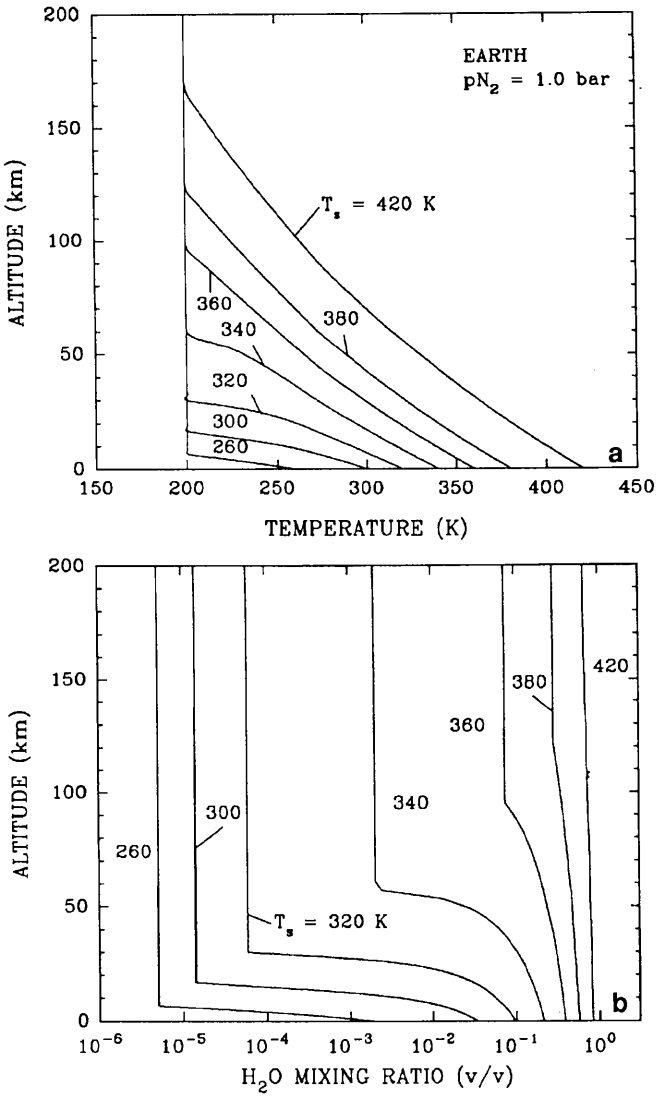

FIG. 2. Vertical profiles of temperature (a) and water vapor mixing ratio (b) for selected surface temperatures in the standard inner edge model.

surface temperatures because of increased Rayleigh scattering. (Surface pressure increases during this process from 1 bar at low T_s to ~270 bar at high T_s.) The planetary albedo, of course, behaves in the opposite manner from F_S. As a result of the combined behavior of F_{IR} and F_S, S_{eff} increases monotonically up to the critical point at 647 K, then remains nearly constant up to extremely high surface temperatures. This leads to a well-defined runaway greenhouse limit of $S_{eff} \simeq 1.41$. The corresponding orbital distance, d (= 1 AU/$S_{eff}^{0.5}$), is 0.84 AU.

The water loss limit is encountered at a much lower value of S_{eff} because the vertical distribution of water vapor changes dramatically as the surface temperature is increased. Figure 2 shows temperature and water vapor profiles for selected values of T_s. The tropopause, defined here as the top of the convective layer, moves up from 10 to 170 km as T_s is increased from 280 to 420 K (Fig. 2a). At the same time, the mixing ratio of stratospheric water vapor increases from $\sim 10^{-5}$ to near unity (Fig. 2b). A rapid transition from low stratospheric H_2O to high stratospheric H_2O occurs near T_s = 340 K. The reason is that water vapor at this point constitutes ~20% of the lower atmosphere. As shown by Ingersoll (1969), "cold-trapping" of water vapor at the tropopause becomes ineffective when the surface water vapor mixing ratio exceeds this critical value.

The results depicted in Figs. 1 and 2 can be convolved to give the mixing ratio of stratospheric water vapor, $f(H_2O)$, as a function of S_{eff} (Fig. 3). This figure can be used to estimate the water loss limit. The diffusion-limited escape rate for hydrogen atoms can be written as (Hunten 1973, Walker 1977)

$$\Phi_{esc}(H) \simeq 2 \times 10^{13} f_t(H) \quad \text{cm}^{-2}\,\text{sec}^{-1}, \tag{8}$$

where $f_t(H)$ ($\simeq 2f(H_2O)$ in this case) is the total hydrogen mixing ratio in the stratosphere. The numerical factor in this equation depends on the atmospheric composition and scale height at the homopause (~100 km altitude), but it should give results that are correct to within a factor of 2 or 3 for most Earth-like planets. Since there are roughly 2×10^{28} H atoms cm^{-2} in the Earth's oceans, the time scale for water loss approaches the age of the Earth for $f(H_2O) \simeq 3 \times 10^{-3}$. Thus, the water loss limit occurs at $S_{eff} \simeq 1.1$ (d = 0.95 AU). As mentioned previously, both this value and the value quoted for the run-

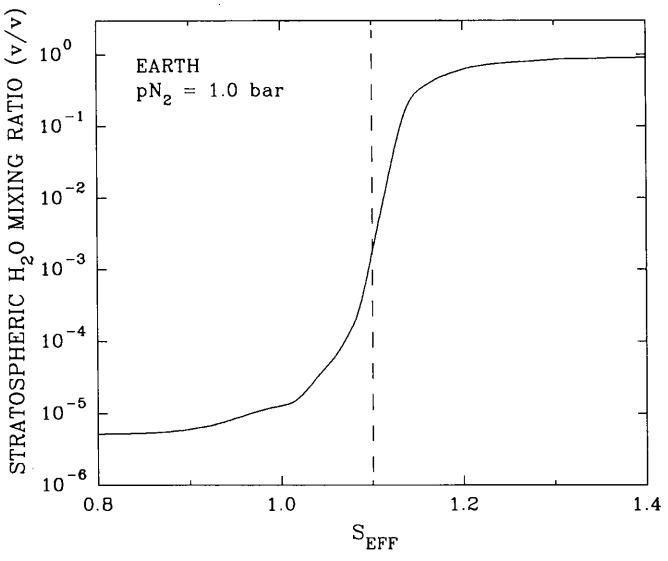

FIG. 3. Variation of stratospheric H_2O mixing ratio with effective solar flux in the standard inner edge model.

away greenhouse limit are conservative because they ignore the possible negative feedback of clouds. The actual inner edge of the HZ around our Sun probably lies at a considerably higher value of S_{eff}.

Outer edge. Model calculations for the outer edge of the HZ are shown in Figs. 4–7. In these calculations, the surface temperature of the "Earth" was fixed at 273 K and the atmospheric CO_2 partial pressure was varied from 1 to 34.7 bars (the saturation vapor pressure for CO_2 at that temperature). Incident and outgoing radiation fluxes were calculated in the same manner as above. The outgoing infrared flux decreases at first as pCO_2 increases to ~10 bars, then approaches a nearly constant value at higher surface pressures (Fig. 4a). The initial decrease is a measure of the greenhouse effect of CO_2; the asymptotic limit is reached when the atmosphere becomes opaque at all infrared wavelengths. The absorbed solar flux decreases with increasing pCO_2 as a consequence of increased Rayleigh scattering. Equivalently, the planetary albedo becomes very high at high CO_2 partial pressures (Fig. 4b). The solar and infrared effects work in opposite directions, causing S_{eff} to reach a minimum value of ~0.36 near pCO_2 = 8 bars (Fig. 4c). This value, which corresponds to d = 1.67 AU, defines the maximum greenhouse limit on the outer edge of the HZ. It is an optimistic outer limit in one sense because it neglects the radiative effect of CO_2 clouds, which are present throughout this calculation (see below). On the other hand, the derived limit on S_{eff} is pessimistic in the sense that it is higher than the effective solar flux for early Mars (S_{eff} = 0.32). As mentioned earlier, one explanation for this apparent discrepancy is that early Mars may have had other greenhouse gases in its atmosphere in addition to CO_2 and H_2O. The same could be true of planets around other stars; this needs to be borne in mind when considering the implications of these results.

Additional physical insight into the behavior of the computer model can be derived by examining the vertical temperature profiles calculated in this sequence (Fig. 5). At pCO_2 = 1 bar, no CO_2 condensation occurs: the temperature profile goes directly from a relatively steep, moist H_2O adiabat in the troposphere to the isothermal stratosphere. At higher CO_2 partial pressures, a region of CO_2 condensation appears in the upper troposphere, where the convective lapse rate is reduced to the much lower value of a moist CO_2 adiabat. At pCO_2 = 34.7 bars, the moist CO_2 adiabat extends all the way down to the surface. The slope discontinuity near 216 K (8 km) is caused by a change in the condensate from CO_2 ice to CO_2 liquid. The very deep condensation regions present at high CO_2 partial pressures would presumably be filled with CO_2 clouds.

A more conservative estimate for the outer edge of the

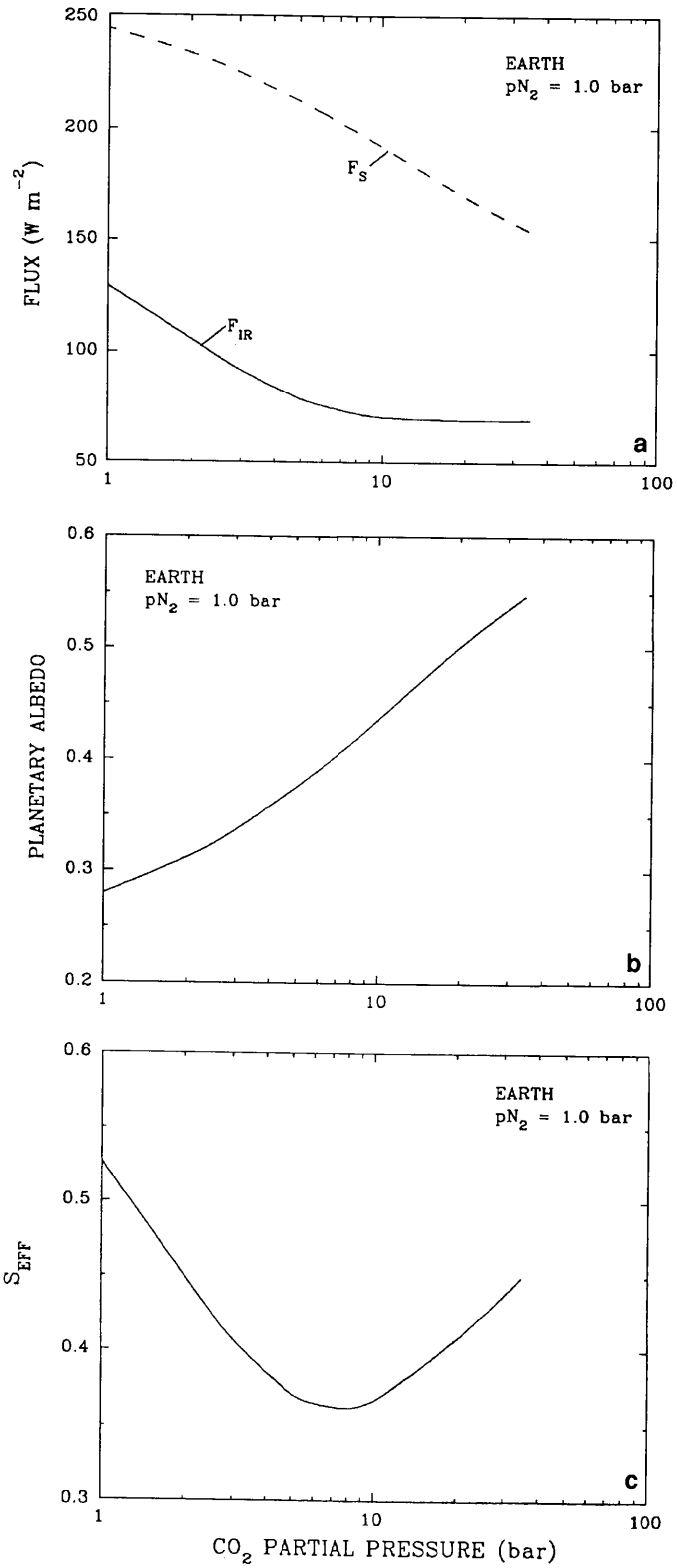

FIG. 4. Dependence of various quantities on atmospheric CO_2 partial pressure for the standard outer edge model: (a) outgoing infrared flux and net incident solar flux, (b) planetary albedo, and (c) effective solar flux. The surface temperature is fixed at 0°C. The curves terminate at pCO_2 = 34.7 bars, the saturation vapor pressure at that temperature.

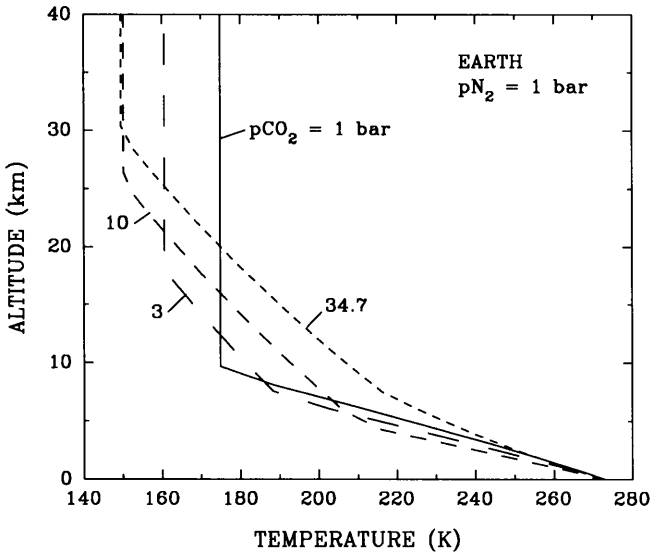

FIG. 5. Vertical temperature profiles for selected CO_2 partial pressures in the standard outer edge model.

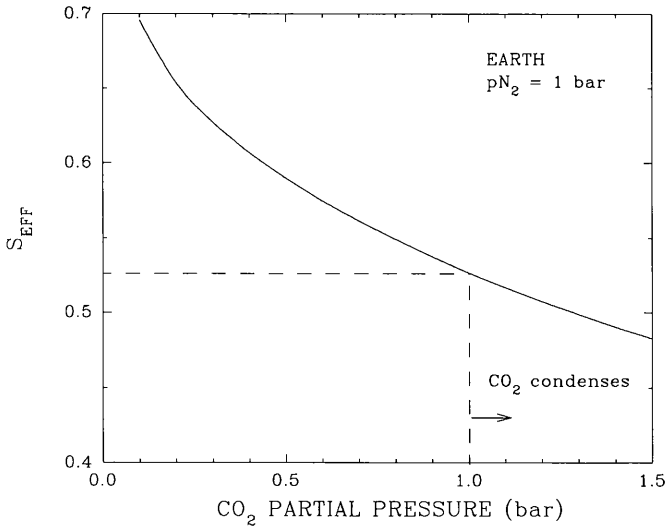

FIG. 7. The variation of effective solar flux with pCO_2 for the sequence of calculations shown in Fig. 6. The dashed lines show where CO_2 first condenses.

HZ is obtained by searching for the minimum CO_2 partial pressure at which CO_2 condenses. Figure 6 illustrates how this limit is derived. The solid curves show the CO_2 volume mixing ratio for different CO_2 partial pressures. The dashed curves show the ratio of P_{sat}/P, that is, the saturation vapor pressure of CO_2 divided by the ambient pressure. The two sets of curves converge at a height of 10 km for pCO_2 just in excess of 1 bar; this marks the point of first CO_2 condensation. Since the effective solar flux is determined as part of the calculation, the corresponding value of S_{eff} is found at the same time (Fig. 7). This procedure yields a 1st condensation limit of S_{eff} = 0.53 (d = 1.37 AU). This value is probably overly pessimistic since the CO_2 clouds formed in such an atmosphere would presumably be very tenuous and would have only a marginal effect on the planetary radiation budget. Our best guess based on this theoretical model alone is that the actual outer edge of the HZ lies somewhere between this limit and the maximum greenhouse limit.

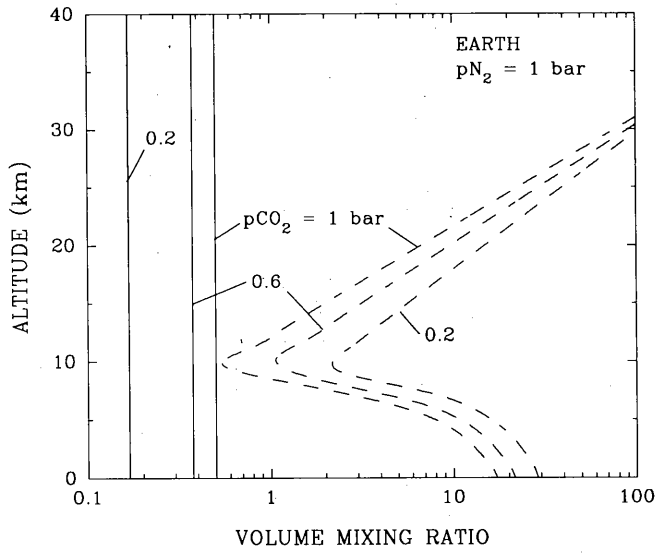

FIG. 6. Diagram illustrating the onset of CO_2 condensation in the standard outer edge model. Solid curves represent the CO_2 volume mixing ratio; dashed curves represent the saturation vapor pressure of CO_2 divided by the ambient atmospheric pressure.

(ii) Computational Uncertainties

A critical assumption made in these calculations is that the stratosphere can be approximated as being isothermal. One can, and should, ask how much effect this has on the results. For the runaway greenhouse and maximum greenhouse limits, the answer is "not much." In the first case, the stratosphere is so tenuous that it is practically transparent to infrared radiation; in the second case it is so cold that little infrared energy is emitted. An increase in T_{strat} of ~50 K is required to change F_{IR} appreciably in a runaway greenhouse atmosphere (Kasting 1988, Fig. 3), while an increase of ~30 K is needed to do this in a maximum greenhouse atmosphere. The stratospheric temperatures assumed here are probably accurate to within this range, so these two habitability limits are in this sense robust. The other two limits are much more sensitive to stratospheric temperature. High values of T_{strat} reduce the effectiveness of the tropopause cold trap, allowing more water vapor to reach the stratosphere. A 40 K increase in T_{strat} would push the water loss limit

from 0.95 AU out to 1.0 AU. Similarly, the onset of CO_2 condensation near the outer edge of the HZ depends strongly on stratospheric temperature. A 20 K decrease in T_{strat} would move the 1st condensation limit in from 1.37 AU to 1.27 AU; a 20 K increase would move the condensation limit out to 1.47 AU. We conclude that these latter two habitability limits are fairly soft. Our predictions might be improved upon by using a climate model that was capable of calculating an accurate stratospheric temperature profile and by taking latitudinal temperature variations into account.

The most serious problem with our climate model, though, is clearly its treatment (or lack thereof) of clouds. This problem has already been addressed to some extent in Section 3. Two different types of clouds must be considered: H_2O clouds, which are probably most important near the inner edge of the HZ, and CO_2 clouds, which are only important near the outer edge of the HZ. Our model approximates the radiative effect of H_2O clouds by placing the cloud layer at the surface and holding the surface albedo invariant. This assumption may seriously underestimate the clouds' effect on planetary albedo at high surface temperatures when the troposphere extends many scale heights above the ground. We can tolerate this uncertainty, however, since it means that our estimates for the inner edge of the HZ are conservative: planets are probably more stable against water loss than our climate model would suggest. The CO_2 clouds near the outer edge are a more vexing problem. We have tried to be conservative by estimating the distance at which these clouds would first form and using this as one of our outer edge limits. However, our climate model is admittedly poor at predicting this distance because the stratospheric temperature is not accurately calculated. Furthermore, our model is only one-dimensional and it is conceivable that CO_2 condensation in the polar regions of a planet would begin to destabilize the climate well before our model would predict (Caldeira and Kasting 1992).

(iii) *Non-Earth-like Planets*

The same calculations can be performed for planets that differ from Earth in various ways, for example, size. To examine this effect, the calculations of Section 5(i) were repeated for planets with surface gravities of 3.73 and 25 m sec^{-2}, as compared to 9.8 m sec^{-2} for Earth. The lower value is the surface gravity of Mars, which has about one-tenth the mass of Earth; the higher value corresponds to a planet about 10 times the mass of Earth. Both planets were assumed to have $pN_2 = 1$ bar. (This assumption may be physically unrealistic because it puts proportionately more nitrogen on the smaller planet than on the big one.) The effect on the four theoretical habitability limits is shown in Table I. All values except for the maximum greenhouse limit change by substantial amounts. In terms of orbital distance, the habitability limits move outward for the Mars-sized planet and inward for the large planet. The reason is that the atmosphere of the Mars-sized planet has a larger column depth, which increases both the planetary albedo and the greenhouse effect. Near the inner edge of the HZ, and at low pCO_2 values near the outer edge, the increased greenhouse effect dominates; at high pCO_2 levels near the outer edge, the increased albedo dominates. The maximum greenhouse limit changes very little because it represents a trade-off between the two competing effects. Since the inner edge moves inward while at least one estimate of the outer edge remains fixed we conclude that, for a given surface pressure, large planets may have somewhat wider HZs than do small ones.

TABLE I
Critical Orbital Distances around Our Sun for Different Planetary Parameters

	Inner edge		Outer edge	
Case	Runaway greenhouse	Water loss	1st CO_2 condensation	Maximum greenhouse
Standard model	0.84	0.95	1.37	1.67
Mars-sized planet*	0.88	0.98	1.49	1.67
Big planet**	0.81	0.91	1.29	1.64
pN_2 = 0.1 bar	0.84	0.96	1.36	1.67
pN_2 = 10 bars	0.84	0.88	1.39	1.69
$pCO_2 = 3 \times 10^{-5}$ bar	0.84	0.94		
$pCO_2 = 3 \times 10^{-3}$ bar	0.84	0.97		
$pCO_2 = 3 \times 10^{-2}$ bar	0.84	0.99		
pCO_2 = 0.3 bar	0.84	1.00		
pCO_2 = 3 bar	0.84	0.95		
pCO_2 = 30 bar	0.84	0.90		

* Surface gravity = 3.73 m sec^{-2}.
** Surface gravity = 25.0 m sec^{-2}.

The habitability advantages of large planets are not limited to the factors mentioned above. Large planets are better able to hold onto their atmospheres over time because their stronger gravitational attraction makes it more difficult for molecules to escape to space. On Earth, the only atoms that escape at significant rates are H and He. In contrast, Mars also loses C, N, and O at rates sufficient to deplete their atmospheric inventories over geologic time (McElroy 1972). Thus, to retain its atmosphere over long time periods a planet probably needs to be several times more massive than Mars. Large planets also have higher internal heat flows and should therefore

be able to maintain tectonic activity on their surfaces for longer periods of time. Tectonic activity of some sort is essential to reprocess carbonate rocks and return CO_2 to the atmosphere. Earth has been able to do this throughout its lifetime, whereas Mars has been geologically dead for perhaps two billion years. Again, this implication is that a planet needs to be several times bigger than Mars to remain habitable for long time periods.

Another factor that might change from one planet to another is atmospheric nitrogen abundance. Changes in pN_2 affect habitability limits by altering the planetary albedo and by influencing the greenhouse effect through pressure broadening of H_2O and CO_2 absorption lines. Table I shows the effect of increasing or decreasing pN_2 by a factor of 10 for an Earth-sized planet. The runaway greenhouse and maximum greenhouse limits are virtually unchanged. Both of these limits are reached in dense atmospheres in which the presence of nitrogen is not that important. In less dense atmospheres, variations in pN_2 have a bigger effect. For example, in the outer edge calculation at $pCO_2 = 1$ bar, increasing pN_2 from 1 to 10 bars reduces F_{IR} by ~35%, increases A_p by ~50%, and reduces the CO_2 partial pressure at which CO_2 clouds begin to form by a factor of 2.5. Surprisingly, the 1st condensation limit changes very little. The invariance of this limit to pN_2 appears to be accidental. Nitrogen abundance does, however, have a significant effect on the water loss limit for the HZ inner edge. Since stratospheric water vapor becomes abundant only when the ground level H_2O mixing ratio exceeds ~20%, increasing pN_2 stabilizes atmospheric water vapor by dilution. A planet with no N_2 and low pCO_2 would be extremely susceptible to water loss. Fortunately, the destabilizing effect of decreasing pN_2 is not seen until extremely low pN_2 values (<0.1 bar). We conclude that planets with high N_2 partial pressures should have wider habitable zones than planets with low pN_2.

Finally, the inner edge of the HZ could be affected by changes in the abundance of atmospheric CO_2. (Such changes are already factored into our estimate for the outer edge.) For example, some planets might have larger total CO_2 endowments or less land area available for weathering. Uninhabited planets might have higher pCO_2 because the silicate weathering rate could be depressed by the absence of the terrestrial biota (Lovelock and Whitfield 1982, Schwartzman and Volk 1989). Changes in pCO_2 would have little effect on the runaway greenhouse limit because that limit is reached in a massive, H_2O-dominated atmosphere. The water loss limit is affected, though; increasing pCO_2 facilitates water loss by raising the surface temperature and increasing the surface H_2O mixing ratio. Table I shows that the maximum destabilization occurs at $pCO_2 \simeq 0.3$ bars, or ~1000 times the present terrestrial CO_2 level. Earth is marginally unstable against water loss at this CO_2 partial pressure. (The calculated critical distance is 1.00 AU.) At higher values of pCO_2, the increase in surface pressure outstrips the increase in the saturation vapor pressure of water, so the atmosphere actually becomes more stable against water loss. This somewhat counterintuitive result was demonstrated previously by Kasting and Ackerman (1986). We conclude that planets with minimum CO_2 partial pressures of a few tenths of a bar have narrower habitable zones than planets, like Earth, where pCO_2 can be reduced to much lower values by the carbonate–silicate cycle.

(iv) *Biological Influences on Planetary Habitability*

Whether or not a planet is inhabited can affect other things besides atmospheric pCO_2. Lovelock (1991) has argued that Earth would have lost both its atmospheric N_2 and its water if not for the activities of the biota. The N_2 would have been converted to nitrate in the oceans and the water would have been lost by outgassing of reduced gases followed by escape of hydrogen to space. (The reduced gases would presumably be produced by reduction of water in the mantle.) Although each of these arguments has some basis, neither appears to preclude the possibility that a lifeless planet could remain habitable. The current rate of NO generation by lightning, ~2.6 Mtons (N) $year^{-1}$ (Borucki and Chameides 1984), is enough to remove all of the atmospheric N_2 in about 1.6 Gyr. The rate of NO generation in an O_2-free atmosphere would be less than half this value (Kasting 1990). Currently, nitrogen is returned to the atmosphere by denitrifying bacteria in the oceans and in sediments. In the absence of bacteria, the most likely return mechanism would involve reduction of nitrate during circulation through mid-ocean ridge hydrothermal systems (Lovelock 1991). Given that there are 1.4×10^{20} moles of N_2 in the atmosphere and that the entire ocean (1.4×10^{21} liters) circulates through axial mid-ocean ridge systems every 10 Myr (Wolery and Sleep 1976, Walker 1985), one can estimate that less than 0.6% of Earth's nitrogen would reside in the oceans in abiotic steady state. So, N_2 would still be a major atmospheric constituent on a lifeless Earth.

Lovelock's argument that an abiotic Earth would have lost its water is based on the idea that hydrogen escape would be much faster if the atmosphere lacked free O_2 and if sulfur-metabolizing bacteria were absent from deep ocean sediments. (The sulfur-metabolizing bacteria might reduce hydrogen loss by combining H_2 with sulfur to form H_2S.) It is certainly true that a low-oxygen atmosphere would have a higher hydrogen escape rate. Photochemical model calculations indicate that most of the H_2 released from volcanos should escape under these circumstances,

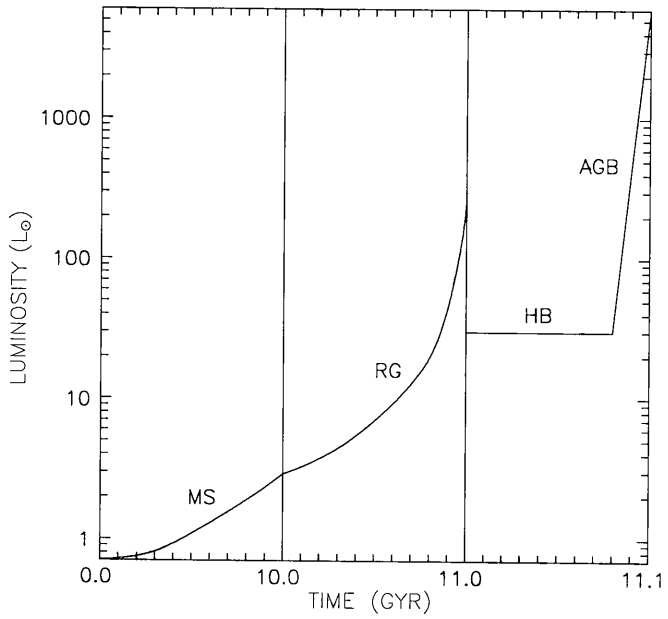

FIG. 8. Luminosity evolution of a $1M_\odot$ star of solar composition, according to models of Iben cited in the text. Note the changes of the time scale at 10 and 11 Gyr. The discontinuity at 11 Gyr is caused by the helium flash. The phases are MS, main sequence; RG, red giant; HB, horizontal branch; AGB, asymptotic giant branch. The final white dwarf phase is not shown. Details of the evolution during the HB and AGB phases are omitted.

as would the additional H_2 produced by photochemical oxidation of CO and SO_2 (Kasting 1990). An upper limit to the potential hydrogen loss rate today can be obtained by taking the combined outgassing rate of these gases, 1.6×10^{12} moles year^{-1} (Holland 1978), and assuming that every molecule outgassed results in the escape of one H_2 molecule. The resulting escape rate would remove an ocean's equivalent of hydrogen in about 50 Gyr. Thus, the ocean would be marginally stable under these circumstances, given present volcanic outgassing rates. We conclude that while biotic activity may indeed help a planet to retain its water, a lifeless Earth would not necessarily be dry.

(v) *The CHZ for Our Sun*

The discussion to this point has concerned the width of the HZ at a given instant in time. But theoretical models of solar evolution predict that the Sun increases in luminosity as it ages (Iben 1967a,b, 1974, Newman and Rood 1977, Gough 1981, Iben and Renzini 1983, Gilliland 1989). Figure 8, which is based on Iben's calculations, shows the predicted luminosity of a solar-type star prior to the time when it becomes a white dwarf. The part that we are concerned with here is the ~10 Gyr main sequence lifetime, during which solar luminosity increases from 0.71 times the present value, L_0, to ~3 times that value. The Sun's luminosity will ultimately soar to ~300 L_0 during its first red giant stage and ~6000 L_0 during its second red giant, or AGB, phase. This may offer some transient possibilities for habitation on the moons of the outer planets, but we view this as less interesting than what goes on earlier in the inner Solar System.

Figure 9a shows how the HZ inner and outer boundaries migrate outward with time for an Earth-like planet, according to Iben's solar evolution model. The three sets of curves for each boundary correspond to the three different habitability limits discussed previously. The calculations

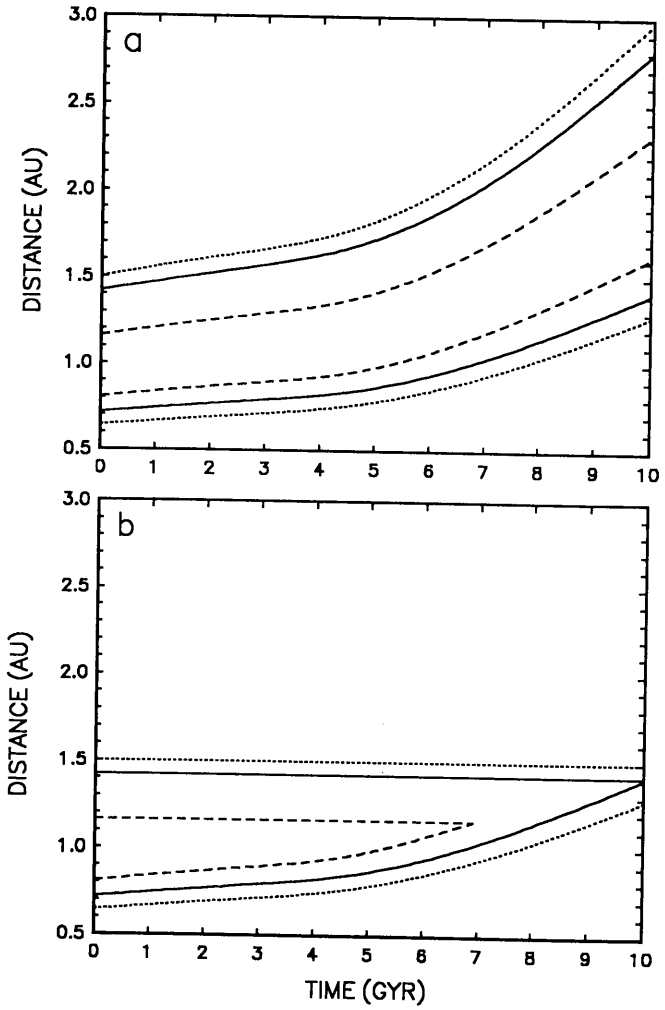

FIG. 9. Evolution of the HZ around a $1M_\odot$ star for two different assumptions concerning the possibility of planetary "cold starts": (a) cold starts permitted, (b) no cold starts allowed. The term cold start refers to whether or not a planet that is initially beyond the outer edge of the HZ will warm up once the stellar luminosity increases to the appropriate critical value. The three pairs of curves correspond to the different habitability estimates discussed in the text: long dashes, "water loss" and "1st CO_2 condensation" limits (most conservative); solid curves, "runaway" and "maximum greenhouse" limits; dotted curves, "recent Venus" and "early Mars" limits (most optimistic).

take into account both the change in the Sun's energy output and the change in its effective temperature. The effect of changes in the wavelength distribution of sunlight is discussed in the next section.

The time evolution of the HZ shown in Fig. 9a is based on the assumption that a planet which is initially beyond the outer edge of the HZ will thaw out once the solar flux reaches the critical value that we have bracketed with our calculations. As discussed by Caldeira and Kasting (1992), this assumption may not be valid. A planet that formed beyond the outer boundary of the HZ would develop a blanket of water ice that would increase the planetary albedo. This ice blanket would eventually become dirty, decreasing the surface albedo (Endal and Schatten 1982), but by then the damage to the planet's climate may already be irreversible. The initial cooling would likely be accompanied by the formation of thick, highly reflective, CO_2 clouds that would not go away even if the surface darkened. Thus, a planet that began its existence in a state of global glaciation might remain that way even when the solar flux had increased well beyond our estimated critical value. Speaking colloquially, it may be impossible to "cold start" a planet without a truly massive input of solar energy. If planetary cold starts are ruled out, the time evolution of the HZ would be similar to the diagram shown in Fig. 9b, in which the outer edge of the HZ is assumed to remain fixed. Note that in this case the HZ disappears entirely after ~7 Gyr if one uses the conservative estimates for the inner and outer edges.

The diagrams shown in Fig. 9 can be used to estimate the width of the CHZ if one first specifies the length of time that a planet is required to remain habitable. We postpone discussion of the general question of CHZs until the next section. A simple calculation, however, gives the answer for the case of 4.6 Gyr of habitability and no cold starts. If we assume that the initial solar luminosity was ~70% of its present value (Gough 1981), the S_{eff} values for the outer edge of the CHZ can be derived by dividing the HZ values by 0.7. The corresponding orbital distances for the 1st condensation, maximum greenhouse, and "early Mars" limits are 1.15, 1.39, and 1.48 AU, respectively. The early Mars limit is slightly less than the actual orbital distance of Mars because the climate constraint is imposed at 3.8 Gyr ago. The inner edge limits for the CHZ are the same as those for the current HZ unless one requires that the Earth remain habitable in the future. Thus, the calculated width of the 4.6-Gyr CHZ is somewhere between 0.2 and 0.76 AU, depending on which habitability limits one chooses. Even our most conservative estimate is three or four times the width of Hart's CHZ [0.06 AU (Hart 1978), 0.046 AU (Hart 1979)]. If other planetary systems have orbital spacings similar to that of our Solar System [Section 6(iii)], the chances of finding habitable planets around solar-type stars seem relatively good.

TABLE II
Stellar Parameters

Stellar type	T_{eff}	$M/M_\odot$	$L/L_\odot$*
M0	3700	0.5	0.06
G2	5700	1.0	1.0
F0	7200	1.3	4.3

* Luminosities represent estimated values midway through a star's main sequence lifetime.

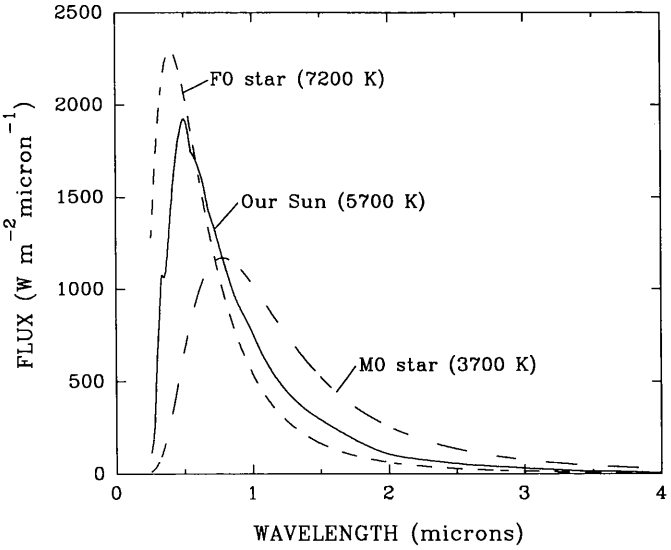

FIG. 10. Spectral energy distributions for our Sun and for two different stars. The dashed curves are blackbody curves; the solid curve is based on observations. All curves are normalized to an integrated solar flux of 1360 W m^{-2}.

6. HABITABLE ZONES AROUND OTHER STARS

(i) *Time Independent Results*

Our Sun, a G2 star, has an effective radiating temperature, T_{eff}, of ~5700 K and outputs its peak energy at a wavelength of ~0.51 μm, according to Wien's Law [$\lambda_{max}(\mu m) = 2898/T$]. The first question that one might ask is how a change in the wavelength of the emitted radiation would affect the limits of the HZ. To answer this question, calculations similar to those described above were performed for an F0 star (T_{eff} ~ 7200 K) and for an M0 star (T_{eff} ~ 3700 K). Approximate masses and luminosities for these stars are given in Table II. The emission from these stars was approximated as blackbody radiation (Fig. 10). To simplify intercomparison, the total

energy flux over the wavelength range of the model (0.24–4.5 μm) was normalized to 1360 W m^{-2}, the present solar constant for Earth. Thus, any differences in the calculated values of S_{eff} compared to those for our Sun are entirely attributable to changes in the wavelength of the incident starlight. Differences in calculated orbital distances include both the wavelength dependence of the starlight and the luminosity of the star.

The results of these calculations are shown in Figs. 11 to 13. Figures 11a (for the inner edge) and 13a (for the outer edge) show that the albedo of an Earth-like planet is higher if its primary is an F0 star and lower if its primary is an M0 star. The reason is twofold: First, the cross section for Rayleigh scattering is proportional to $1/\lambda^4$, so diffuse reflection increases as the incident radiation is blue-shifted. And, second, the absorption coefficients of H_2O and CO_2 are much stronger in the near-infrared than in the visible, so the amount of starlight absorbed by the planet's atmosphere increases as the radiation is red-shifted. Both effects are most pronounced when the atmosphere is dense and full of gaseous absorbers; hence, the albedo differences are largest at high planetary temperatures (Fig. 11a) or at high CO_2 partial pressures (Fig. 13a).

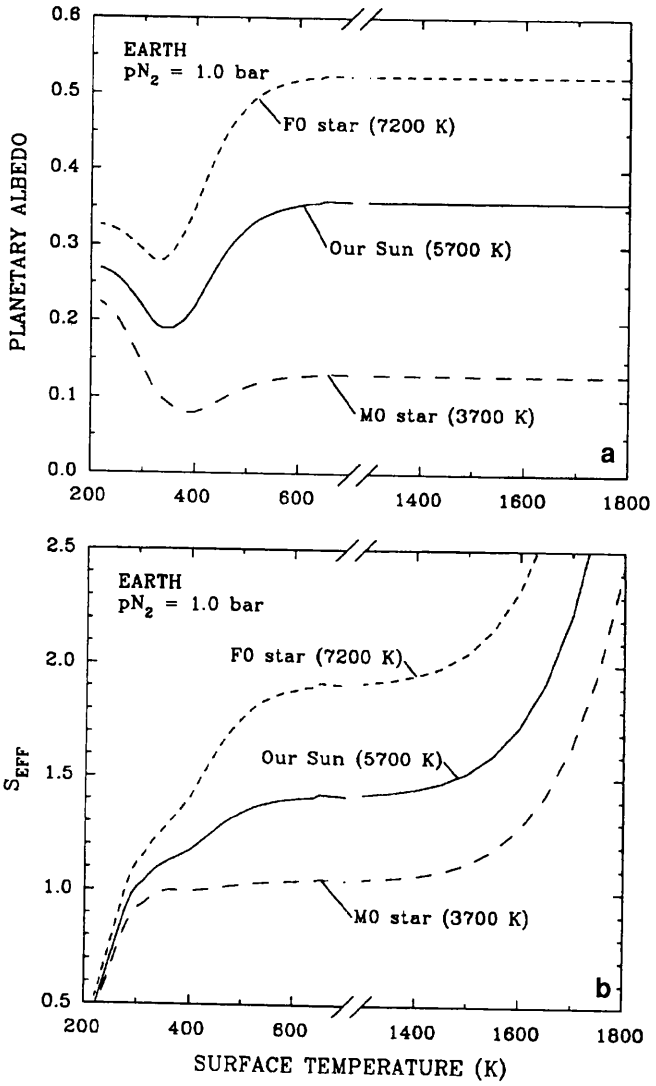

FIG. 11. Planetary albedo (a) and effective solar flux (b) as a function of surface temperature in the inner edge model for the three different stars shown in Fig. 10.

TABLE III
Critical Solar Fluxes and Orbital Distances for Different Stellar Types

	M0		G2		F0	
Limit	S_{eff}	AU	S_{eff}	AU	S_{eff}	AU
Recent Venus*	1.60	0.19	1.76	0.75	2.00	1.47
Runaway greenhouse	1.05	0.24	1.41	0.84	1.90	1.50
Water loss	1.00	0.25	1.10	0.95	1.25	1.85
1st CO_2 condensation	0.46	0.36	0.53	1.37	0.61	2.70
Maximum greenhouse	0.27	0.47	0.36	1.67	0.46	3.06
Early Mars**	0.24	0.50	0.32	1.77	0.41	3.24

* Recent Venus limits for M0 and F0 stars scaled by S_{eff} for water loss.

** Early Mars limits for M0 and F0 stars scaled by S_{eff} for maximum greenhouse.

These changes in planetary albedo affect the boundaries of the HZ in predictable ways. Critical solar fluxes and orbital distances for the different habitability limits are given in Table III. At the inner edge, the runaway greenhouse limit on S_{eff} increases by roughly 30% for an F0 star and decreases by approximately the same amount for an M0 star (Fig. 11b). The water loss limit changes by about $\pm 10\%$ in the same directions (Fig. 12). At the outer edge, the maximum greenhouse limit changes by about $\pm 30\%$ (Fig. 13b) while the 1st condensation limit (not shown) changes by about $\pm 15\%$, all values being higher for the F0 star and lower for the M0 star. As discussed in Section 3, two additional estimates for the boundaries of the HZ can be derived from recent Venus and early Mars. These limits were extrapolated to other stellar types by scaling the Venus limit by the corresponding values of S_{eff} for water loss and the early Mars limit by S_{eff} for the maximum greenhouse effect. Orbital distances corresponding to the various values of S_{eff} were computed using the inverse square law

$$d = 1\ \text{AU} \left(\frac{L/L_\odot}{S_{\text{eff}}} \right)^{0.5}, \qquad (9)$$

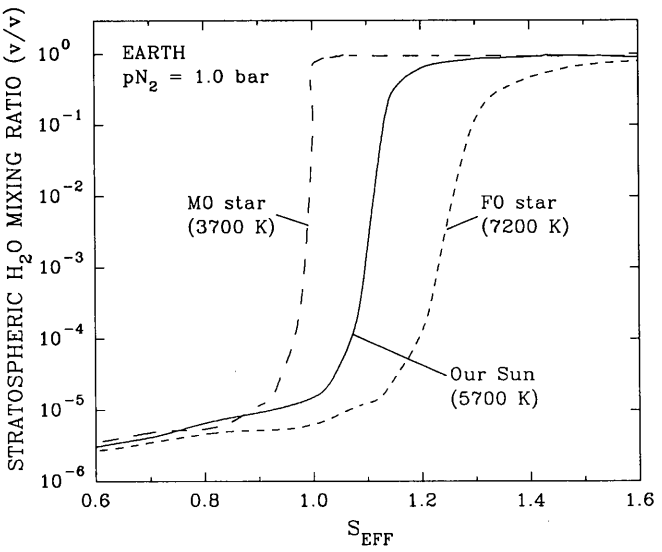

FIG. 12. Stratospheric water vapor mixing ratio as a function of effective solar flux in the inner edge model for the three stars shown in Fig. 10.

where $L/L_\odot$ represents the luminosity of the star compared to that of our Sun.

(ii) Time Dependent Results

The calculations of the previous subsection can be used in conjunction with stellar evolution models for stars of different masses to estimate the time evolution of their HZs (Fig. 14). To simplify the figure, we show only the intermediate estimates (i.e., the runaway and maximum greenhouse limits) for the HZ boundaries. As in Fig. 9, results are shown for the case where cold starts are allowed (Fig. 14a) or ruled out (Fig. 14b). Stellar luminosities and effective temperatures for these calculations were taken directly from Iben (1967a,b) for masses 1.25 and 1.5 $M_\odot$. Since Iben's $1M_\odot$ star does not precisely reproduce the Sun's present luminosity, we have constrained it to be consistent with the model of Gough (1981) for times between 0 and 4.6 Gyr. For the slowly evolving $0.5M_\odot$ and $0.75M_\odot$ stars, Iben does not present complete evolutionary tracks; hence, we used his ZAMS (zero-age-main-sequence) luminosities, temperatures, and main sequence lifetimes to generate our own models. The critical fluxes for the different habitability limits were corrected for stellar temperature by quadratically fitting the values of S_{eff} listed in Table III. The results shown in Fig. 14b (the "no cold starts" case) are convolved in Fig. 15 to show the width of the CHZ as a function of stellar mass and the time, τ_H, that a planet is required to remain habitable.

The results shown in Figs. 14 and 15 can be summarized as follows: (i) The width of the CHZ around different stars is strongly dependent on τ_H. Our $1.5M_\odot$ star, a late A star, has a calculated main sequence lifetime of ~2.0 Gyr; hence, it has a finite CHZ only for times shorter than this. Stars much more massive than $1.5M_\odot$ can probably be ruled out as candidates for SETI because life in such a system would not have had sufficient time to evolve intelligence, based on our experience here on Earth. On the other hand, planets orbiting such stars might harbor primitive forms of life and could conceivably be colonized by humans if we ever solve the problem of interstellar travel. A possible problem would be the high ultraviolet flux emanating from such stars, which would require a superefficient ozone screen to allow their planets to be habitable. (ii) The stars with the longest-lived CHZs are the K and M stars. This longevity is a natural consequence of

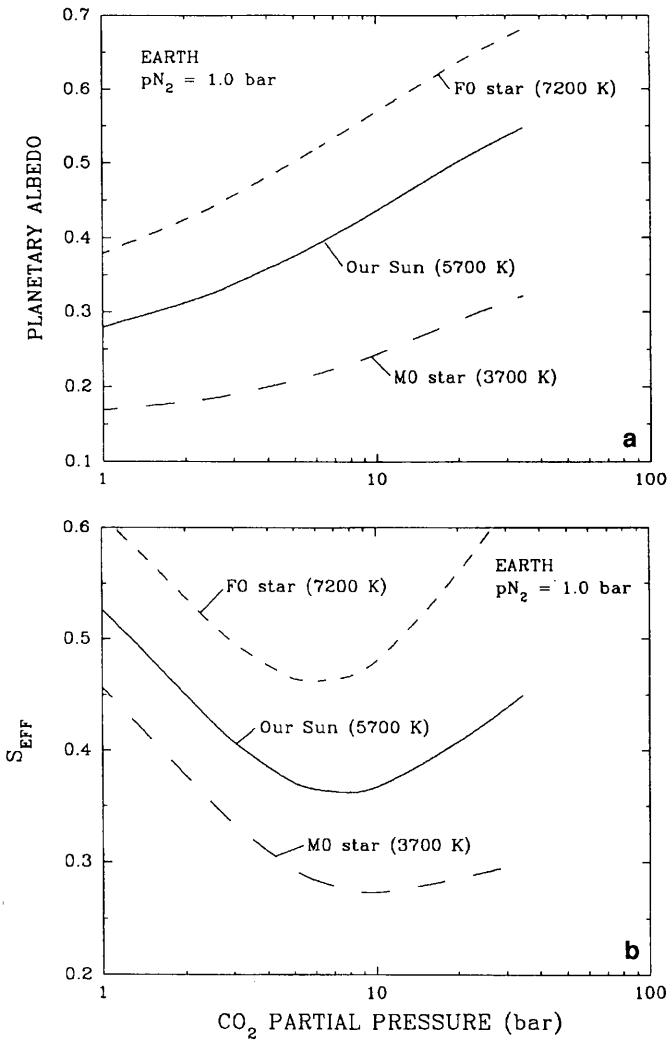

FIG. 13. Planetary albedo (a) and effective solar flux (b) as a function of CO_2 partial pressure in the outer edge model for the three different stars shown in Fig. 10.

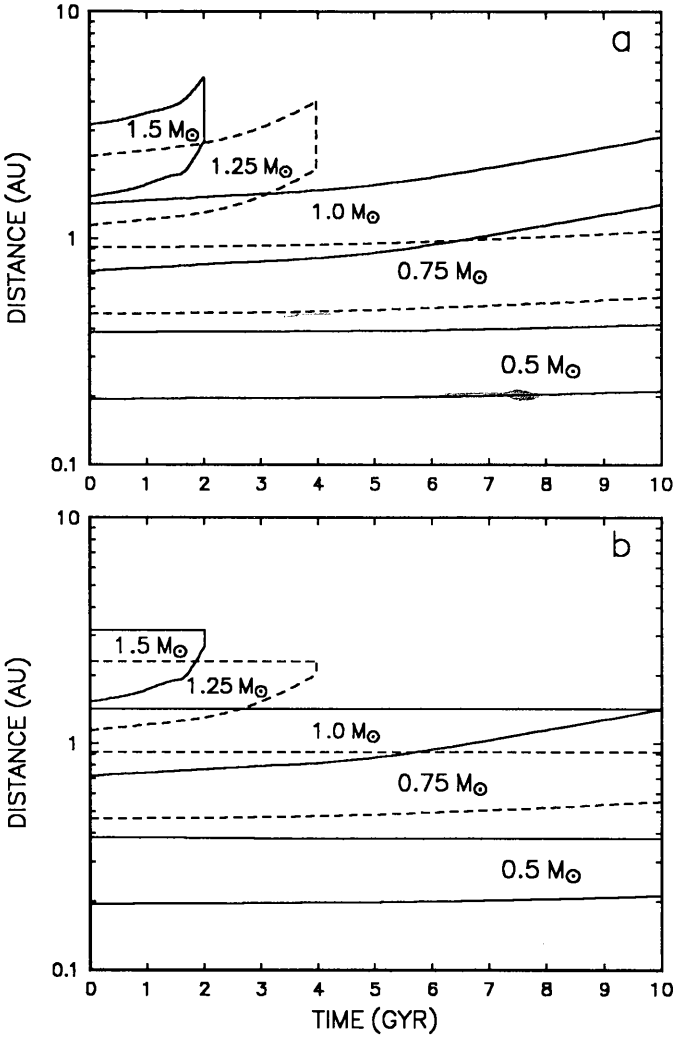

FIG. 14. Evolution of the HZ around different stars for two different assumptions about the possibility of planetary cold starts: (a) cold starts permitted, (b) no cold starts allowed. The intermediate (runaway and maximum greenhouse) estimates for the width of the HZ were used and the evolution was truncated at the end of the main sequence phase.

their slow evolution, which causes the boundaries of the HZ to remain nearly fixed in space. Other factors (discussed below) must be considered, however, before one can evaluate their potential for harboring habitable planets. (iii) All of our calculated CHZs are much broader (4–20 times) than those of Hart (1979). Indeed, Hart concluded that the 4.6-Gyr CHZ disappeared entirely for stars later than K0, corresponding to masses $<0.85\ M_{\odot}$. The reason was that he assumed that all planets lost their reduced greenhouse gases at the same time in their evolution that the Earth's atmosphere became oxidizing, ~2.5 Gyr after planetary formation. In his model, the lower mass stars had not increased much in luminosity by this time, so their planets experienced runaway glaciation. Our model avoids ad hoc assumptions as much as possible.

(iii) Planetary Formation and Spacing

The questions of whether and where planets form around other stars are of central importance to our subject. Support for the idea that planets exist around other stars may be drawn from observations of what appear to be accretion disks around young T-Tauri stars and around some older, main sequence stars (Aumann *et al.* 1984), including G and K types (Backman and Paresce 1992). Taking into account selection effects, it is estimated that at least half of all nearby main sequence stars have significant, nonphotospheric IR excesses at IRAS wavelengths (10–100 μm). These excesses have been interpreted as evidence for disks of orbiting, 1- to 100-μm-size grains. In the case of β Pic the disk has been resolved optically (Smith and Terrile 1984). The estimated lifetime of the grains against various destruction mechanisms is generally less than the age of the star; consequently, the observed grains must have larger sources, presumably planetesimals (Whitmire *et al.* 1988, Backman and Paresce 1992). Extensive modeling of the IRAS data and of observations at different wavelengths indicates that the three prototype systems (α Lyr, α Psa, and β Pic) all have gaps or holes in their inner disks with radii in the range of ~20 to 80 AU. One possible explanation for the maintenance of these gaps against Poynting–Robertson and collisional diffusion is the presence of a planetary system. Thus,

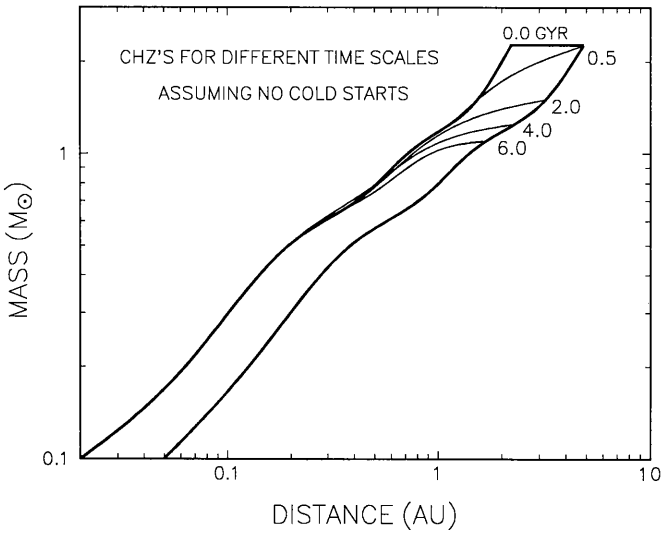

FIG. 15. CHZ widths as a function of stellar mass for different planetary habitability times, τ_H, again using the intermediate HZ limits. The calculations shown here assume that planetary cold starts are not possible; thus, the inner edge of the CHZ moves outward as τ_H increases, but the outer edge remains fixed. The $\tau_H = 0$ outer envelope corresponds to the HZ of a ZAMS star.

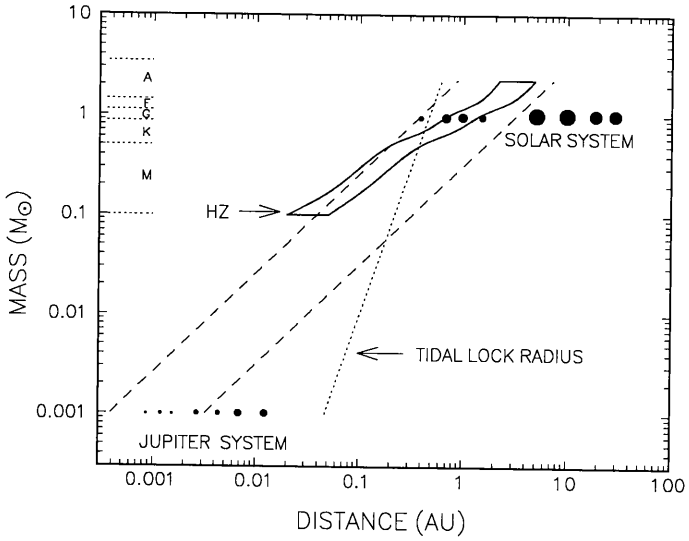

FIG. 16. Diagram showing the ZAMS habitable zone (solid curves) as a function of stellar mass (intermediate habitability estimates used). The long-dashed lines delineate the probable terrestrial planet accretion zone. The dotted line represents the distance at which an Earth-like planet in a circular orbit would be locked into synchronous rotation within 4.5 Gyr as a result of tidal damping. Note that all Earth-like planets within the HZ of an M star would be within this radius.

there is good observational evidence that protoplanetary nebulae are a common feature of star formation, even if direct observations of planets (not counting those around pulsars) are still lacking.

A second issue is that of planetary spacing. As has been recognized for many years, the spacing of planets in our Solar System is quite regular, except for the gap at the asteroid belt. One way of describing this spacing is Bode's Law, in which the orbital distance in AU is given by forming the sequence 4, $4 + (3 \times 2^0)$, $4 + (3 \times 2^1)$, ..., and then dividing the resulting numbers by 10. The explanation for Bode's Law has eluded generations of celestial mechanicians, but it probably involves considerations of orbital stability and/or geometric constraints on planetary accretion. [See discussion and literature references in Isaacman and Sagan (1977), bearing in mind that the computer model they employ is very simple. The recent paper by Sussman and Wisdom (1992) suggests that we may be close to solving the orbital stability problem.] Based on this premise, we have chosen to present our HZ and CHZ results (Figs. 14–16) on a log distance scale. Additional support for this assumption is provided by the observed distribution of the Jovian moons, which also follows this same pattern (Fig. 16). Although its mass is much less than that of a star, Jupiter is thought to have had its own accretion disk and, thus, would be expected to have formed moons in a manner analogous to the way a star would form planets. The relevance of a logarithmic distribution of planets to HZs has been previously noted by Cameron (1963). If one does not make this assumption, then F stars look like the best candidates for harboring habitable planets (at least for short values of τ_H) because their HZs are wide in an absolute sense (Huang 1959, 1960).

In addition to understanding qualitatively how planets are spaced, one needs to be able to predict how big and how far apart they will be. Some progress on these questions has been made in recent numerical simulations of planetary accretion by Wetherill (1991) (and earlier references therein). Wetherill's model predicts an average of 1–2 planets with masses $\geq 0.5\ M_\odot$ forming between 0.6 and 1.4 AU in our own Solar System, similar to what is actually observed. If these results are applicable to other solar-type stars, the probability of forming an Earth-like planet within the 4.6-Gyr CHZ is ~50%, even using our most conservative habitability limits. Wetherill's model forms planets randomly, rather than logarithmically, throughout the inner Solar System, but that may be because his Monte Carlo technique does not automatically include resonances.

Finally, one would like to show that planets will form at the right distance to be within a star's CHZ. For stars much bigger or smaller than the Sun, a simple argument shows that planetary formation distances should scale with stellar mass. Consider the process of grain condensation in an optically thin nebula around a pre-main sequence (PMS) star. In this case the local grain temperature is determined by the balance between the absorbed stellar flux and the emitted infrared flux. The distance at which various compounds condense is determined primarily by the local temperature and is therefore $\propto L_{PMS}^{0.5}$. During the PMS phase the star's luminosity is a consequence of gravitational contraction, which varies as M^2. Thus, the distance at which grains of a given composition condense is proportional to M. The actual situation is more complicated. The nebula would probably be optically thick, so the details of turbulent heat transfer would be important. Nevertheless, the same general trend would be expected: smaller stars should tend to form planets closer in and larger stars ought to form them farther out.

We used the linear scaling law derived above to estimate the terrestrial planet formation region around other stars. This gives rise to the dashed lines shown in Fig. 16. The lower dashed line, which is drawn to pass through our own Solar System at the asteroid belt (3.2 AU), intersects the Jovian system between Io and Europa. Since Io is mostly rock, whereas Europa contains a significant amount of ice, the Jovian system makes the transition from rocky to icy bodies just about where our simple, linear scaling law would predict. Io and several other small, rocky satellites lie well within the extrapolated terrestrial planet accretion zone. The Galilean moons, especially Io and Europa, have undergone some orbital

expansion since their formation, so their original orbits should have been somewhat deeper within this zone.

Also plotted in Fig. 16 are the ZAMS habitable zones for stars of different masses. The HZ lies entirely within the terrestrial planet accretion zone for all stars earlier than ~M0 and partly within it for the M stars. This implies that around most stars the chances of forming planets within the HZ are reasonably good. We would not defend this statement too vigorously, since our assumptions are admittedly crude. Nevertheless, it seems fair to say that there is no reason to expect that the formation of planets within a star's HZ is a rare occurrence.

(iv) Tidal Locking around M Stars

Dole (1964) pointed out that planets orbiting M stars might be synchronously rotating as a result of tidal damping. If one expresses all quantities in CGS units, the tidal radius at which an Earth-like planet in a circular orbit would become tidally locked in a specified amount of time, t, is given by (Peale 1977)

$$r_T = 0.027 \left(\frac{P_0 t}{Q}\right)^{1/6} M^{1/3}. \quad (10)$$

Here, P_0 is the original rotation period of the planet, Q^{-1} is the solid body plus ocean specific dissipation function, and M is the stellar mass. Today, the Earth's Q is relatively low (~13) as a consequence of rapid dissipation of energy in shallow seas. However, a value this small is inconsistent with the evolution of the Earth–Moon system, and the average solid body Q is probably closer to 100 (Burns 1986). We used $Q = 100$, $t = 4.5$ Gyr, and $P_0 = 13.5$ hr to calculate the tidal lock radius as a function of stellar mass, shown as the dotted line in Fig. 16. Fortunately, r_T is relatively insensitive to these parameters.

Figure 16 predicts that Earth-like planets in circular orbits within the HZ of all M stars ($M \leq 0.5\ M_\odot$) would be synchronously rotating after 4.5 Gyr of evolution. Planets near the inner edge of the HZ around late K stars would be subject to this problem as well. Synchronous rotation could result in the permanent freezing of water and other volatiles on the dark hemisphere, rendering such planets uninhabitable. Planets with very dense atmospheres, like Venus, would not have their volatiles cold-trapped in this manner, but they would probably be too hot to be habitable. Of course, synchronous rotation is not the only possible consequence of tidal damping. Mercury, which lies inside the tidal lock radius on our diagram, is trapped in a 3:2 spin–orbit resonance which causes it to rotate nonsynchronously, albeit slowly. A different example of nonsynchronous rotation is illustrated by Venus. Venus' slow retrograde rotation should have damped out in less than 1 Gyr. It is suspected that atmospheric tides have stabilized the rotation rate and prevented synchronous rotation from being achieved (Dobrovolskis 1980). Thus, one should not rule out M stars altogether as possible abodes for life on this basis. The later M stars also exhibit significant flare activity, which might make them very unhealthy to live near. All things considered, M stars rank well below G and K stars in their potential for harboring habitable planets.

(v) Habitable Zones in Multiple Star Systems

To this point we have confined our discussion to single, isolated stars. However, more than 65% of stars in the mass range of interest are believed to be members of binary or multiple star systems (Duquennoy and Mayor 1991). These systems have often been rejected as possible abodes for life. An early objection was based on the belief that planetary orbits in such systems would not be stable for long time periods. That belief has been challenged by Graziani and Black (1981) and Pendleton and Black (1983), who found that stable, circular, planetary orbits could exist, provided that the planet's orbital radius was a factor of 5 or more larger than the binary separation (external case—planet orbits center of mass), or vice versa (internal case—planet orbits single star). Whether a planet could form in such an orbit is, of course, a separate question. Infrared excesses are seen in binaries, as well as in single stars (Backman and Paresce 1992), implying that planets do form in such systems [see Section 6(iii)]. Duquennoy and Mayor (1991) give the distribution of orbital periods and eccentricities for a large group of nearby multiple star systems containing solar-type stars. Using their statistics, the above orbital stability criterion, and our HZ results, we estimate that ~5% of external binaries and ~50% of internal binaries could support habitable planets in stable orbits. Clearly, such systems deserve to be considered as possible abodes for life even if the factors affecting planetary habitability are somewhat more complex than for single stars.

7. CONCLUSIONS

For Earth-like planets orbiting main sequence stars, the HZ is determined by water loss on the inner edge and by CO_2 condensation, leading to runaway glaciation, on the outer edge. Planetary habitability is critically dependent on atmospheric CO_2 and its control by the carbonate–silicate cycle. Conservative estimates for the boundaries of the Sun's current HZ are 0.95 AU for the inner edge and 1.37 AU for the outer edge. The actual HZ width is probably greater, but is difficult to pin down precisely because of uncertainties regarding clouds. HZ widths around other stars in the spectral classification range of interest, F to M, are approximately the same if distances are expressed on a logarithmic scale. If planets exist

around other stars and if planetary spacing is logarithmic, as in our Solar System, the chances that one or more planets will be found within a star's HZ are fairly good.

The width of the CHZ around a star depends on the time that a planet is required to remain habitable and on whether a planet that is initially frozen can be cold-started by a modest increase in stellar luminosity. CHZs are generally narrower than HZs because the boundaries of the HZ migrate outward as a star ages. Despite this, the 4.6-Gyr CHZ around our own Sun extends from at least 0.95 to 1.15 AU and is probably considerably wider. CHZs around early K stars should be somewhat wider (in log distance) than around G stars because the K stars evolve more slowly. Equivalently, one could say that their CHZs are longer-lived. Since there are approximately three times as many K stars as G stars, this suggests that the majority of habitable planets may reside around K stars. Late K stars and M stars would have even wider CHZs based on our climate model, but the planets within them are susceptible to tidal damping and will probably rotate synchronously after a few billion years. F stars should have narrower CHZs than do G stars (again on a log distance scale) because they evolve more rapidly. High ultraviolet fluxes are another potential problem for life around F stars. Stars earlier than ~F0 have main sequence lifetimes of <2 Gyr, so their planets are probably not suited for evolving intelligent life.

Implications for SETI. The current SETI targeted-search strategy (Soderbloom and Latham 1991) is to observe all single stars within 5 pc of the Sun (~60 stars) and all G dwarfs within 50 pc (~1,000 stars). Our results suggest that mid-to-early K dwarfs should be included in this second phase. After these two initial phases of the program, it must be decided whether to prioritize the more distant G stars or the closer, more numerous K stars. Since there will be some disadvantage in signal strength for the more distant G stars, and since mid-to-early K stars appear to be at least as attractive from a climate standpoint, the present study suggests that the K stars should be observed before extending the G star search much beyond 50 pc.

Future work. We have identified several areas in which additional theoretical modeling would be useful. These include multidimensional calculations of atmospheric circulation on synchronously and slowly rotating planets to determine whether their volatiles would be cold-trapped out, the feasibility of planetary cold starts, the radiative effects of CO_2 and H_2O clouds, the puzzle of Mars' early climate, the question of planetary spacing, and the problem of whether habitable planets could exist in multiple star systems. The most important research areas, however, are the observational ones: the direct telescopic search for other planets and SETI. If either of these searches were to succeed, the topic of habitable zones around stars would assume a high level of significance.

ACKNOWLEDGMENTS

The authors thank M. Fogg, J. Matese, and L. Doyle for their helpful comments on this research and on the manuscript. C. Sagan provided constructive criticism during review. JFK's contribution to this research was supported by Grant NAGW-1911 to Penn State University from NASA's Exobiology Program. DPW was supported by a NASA–Ames/Stanford ASEE fellowship and a grant from the Louisiana Educational Quality Support Fund.

Note added in proof. Since this paper was drafted, NASA's SETI project has been revised and is now termed the 'High Resolution Microwave Survey,' or HRMS.

REFERENCES

AUMANN, H. H., *et al.* 1984. Discovery of a shell around Alpha Lyrae. *Astrophys. J.* **278,** L23–L27.

BACKMAN, D. E., AND F. PARESCE 1992. Main sequence stars with circumstellar solid material: The Vega phenomenon. In *Protostars and Planets III,* Univ. of Arizona Press, Tucson.

BERNER, R. A., A. C. LASAGA, AND R. M. GARRELS 1983. The carbonate–siliate geochemical cycle and its effect on atmospheric carbon dioxide over the past 100 million years. *Am. J. Sci.* **283,** 641–683.

BORUCKI, W. J., AND W. L. CHAMEIDES 1984. Lightning: Estimates of the rate of energy dissipation and nitrogen fixation. *Rev. Geophys.* **22,** 363–372.

BUDYKO, M. I. 1969. The effect of solar radiation variations on the climate of the Earth. *Tellus* **21,** 611–619.

BURNS, J. A. 1986. The evolution of satellite orbits. In *Satellites* (J. A. Burns and M. S. Matthews, Eds.), p. 117–158. Univ. of Arizona Press, Tucson.

CALDEIRA, K., AND J. F. KASTING 1992. Susceptibility of the early Earth to glaciation caused by carbon dioxide clouds. *Nature* **359,** 226–228.

CAMERON, A. G. W. 1963. Stellar life zones. In *Interstellar Communication* (A. G. W. Cameron, Ed.), p. 107–114. W. A. Benjamin, New York.

DOBROVOLSKIS, A. 1980. Atmospheric tides and the rotation of Venus. II. Spin evolution. *Icarus* **41,** 18–35.

DOLE, S. H. 1970. Computer simulation of the formation of planetary systems. *Icarus* **13,** 494–508.

DOLE, S. H. 1964. *Habitable Planets for Man.* Blaisdell, New York.

DONAHUE, T. M., AND R. R. HODGES, JR. 1992. The past and present water budget of Venus. *J. Geophys. Res.* **97,** 6083–6091.

DONAHUE, T. M., J. H. HOFFMAN, AND R. R. HODGES, JR. 1982. Venus was wet: A measurement of the ratio of deuterium to hydrogen. *Science* **216,** 630–633.

DUQUENNOY, A., AND M. MAYOR 1991. Multiplicity among solar-type stars in the solar neighborhood. II. Distribution of the orbital elements in an unbiased sample. *Astron. Astrophys.* **248,** 485–524.

FOGG, M. J. 1992. An estimate of the prevalence of biocompatible and habitable planets. *J. Br. Interplanet. Soc.* **45,** 3–12.

GILLILAND, R. L. 1989. Solar evolution. *Global Planet. Change* **1,** 35–55.

GOUGH, D. O. 1981. Solar interior structure and luminosity variations. *Solar Phys.* **74,** 21–34.

GRAZIANI, F., AND D. C. BLACK 1981. Orbital stability constraints on the nature of planetary systems. *Astrophys. J.* **251,** 337–341.

GRINSPOON, D. H. 1987. Was Venus wet? Deuterium reconsidered. *Science* **238,** 1702–1704.

GRINSPOON, D. H., AND J. S. LEWIS 1988. Cometary water on Venus: Implications of stochastic comet impacts. *Icarus* **74,** 430–436.

GURWELL, M. A., AND Y. L. YUNG 1992. Fractionation of hydrogen and deuterium on Venus due to collisional ejection. Planetary Space Sci., in press.

HART, M. H. 1978. The evolution of the atmosphere of the Earth. *Icarus* **33,** 23–39.

HART, M. H. 1979. Habitable zones about main sequence stars. *Icarus* **37,** 351–357.

HOLLAND, H. D. 1978. *The Chemistry of the Atmosphere and Oceans.* Wiley, New York.

HUANG, S.-S. 1960. Life outside the solar system. *Sci. Am.* **202**(4), 55–63.

HUANG, S.-S. 1959. Occurrence of life in the universe. *Am. Sci.* **47,** 397–402.

HUNTEN, D. M. 1973. The escape of light gases from planetary atmospheres. *J. Atmos. Sci.* **30,** 1481–1494.

IBEN, I. 1967a. Stellar evolution within and off the main sequence. *Annu. Rev. Astron. Astrophys.* **5,** 571–626.

IBEN, I. 1967b. Stellar evolution. VI. Evolution from the main sequence to the red-giant branch for stars of mass 1 $M_\odot$, 1.25 $M_\odot$, and 1.5 $M_\odot$. *Astrophys. J.* **147,** 624–649.

IBEN, I. 1974. Post main sequence evolution of single stars. *Annu. Rev. Astron. Astrophys.* **12,** 215–256.

IBEN, I., AND A. RENZINI 1983. Asymptotic giant branch evolution and beyond. *Ann. Rev. Astron. Astrophys.* **21,** 271–342.

INGERSOLL, A. P. 1969. The runaway greenhouse: A histroy of water on Venus. *J. Atmos. Sci.* **26,** 1191–1198.

ISAACMAN, R., AND C. SAGAN 1977. Computer simulations of planetary accretion dynamics: Sensitivity to initial conditions. *Icarus* **31,** 510–533.

KASTING, J. F. 1988. Runaway and moist greenhouse atmospheres and the evolution of Earth and Venus. *Icarus* **74,** 472–494.

KASTING, J. F. 1989. Long-term stability of the Earth's climate. *Palaeogeogr. Palaeoclimat. Palaeoecol.* **75,** 83–95.

KASTING, J. F. 1990. Bolide impacts and the oxidation state of carbon in the Earth's early atmosphere. *Origins of Life* **20,** 199–231.

KASTING, J. F. 1991. CO_2 condensation and the climate of early Mars. *Icarus* **94,** 1–13.

KASTING, J. F., AND J. B. POLLACK 1983. Loss of water from Venus. I. Hydrodynamic escape of hydrogen. *Icarus* **53,** 479–508.

KASTING, J. F., J. B. POLLACK, AND T. P. ACKERMAN 1984. Response of Earth's atmosphere to increases in solar flux and implications for loss of water from Venus. *Icarus* **57,** 335–355.

KASTING, J. F., AND T. P. ACKERMAN 1986. Climatic consequences of very high CO_2 levels in the Earth's early atmosphere. *Science* **234,** 1383–1385.

KASTING, J. F., O. B. TOON, AND J. B. POLLACK 1988. How climate evolved on the terrestrial planets. *Sci. Am.* **256,** 90–97.

KASTING, J. F., AND O. B. TOON 1989. Climate evolution on the terrestrial planets. In *Origin and Evolution of Planetary and Satellite Atmospheres* (S. K. Atreya, J. B. Pollack, M. S. Matthews, Eds.), pp. 423–449. Univ. of Arizona Press, Tucson.

LOVELOCK, J. E., AND M. WHITFIELD 1982. Life span of the biosphere. *Nature* **296,** 561–563.

LOVELOCK, J. E. 1991. *Gaia: The Practical Science of Planetary Medicine.* Gaia Books, London.

MANABE, S., AND R. T. WETHERALD 1967. Thermal equilibrium of the atmosphere with a given distribution of relative humidity. *J. Atmos. Sci.* **24,** 241–259.

MCELROY, M. B. 1972. Mars: An evolving atmosphere. *Science* **175,** 443–445.

NEWMAN, M. J., AND R. T. ROOD 1977. Implications of solar evolution for the Earth's early atmosphere. *Science* **198,** 1035–1037.

NORTH, G. R. 1975. Theory of energy-balance climate models. *J. Atmos. Sci.* **32,** 2033–2043.

PEALE, S. J. 1977. Rotation histories of the natural satellites. In *Planetary Satellites* (J. A. Burns, Ed.). Univ. of Arizona Press, Tucson.

PENDLETON, Y. J., AND D. C. BLACK 1983. Further studies on criteria for the onset of dynamical instability in general three-body systems. *Astron. J.* **88,** 1415–1419.

POLLACK, J. B., J. F. KASTING, S. M. RICHARDSON, AND K. POLIAKOFF 1987. The case for a wet, warm climate on early Mars. *Icarus* **71,** 203–224.

POLLARD, W. G. 1979. The prevalence of Earthlike planets. *Am. Sci.* **67,** 653–659.

RAMANATHAN, V., AND W. COLLINS 1991. Thermodynamic regulation of ocean warming by cirrus clouds deduced from observations of the 1987 El Nino. *Nature* **351,** 27–32.

RASOOL, S. I., AND C. DEBERGH 1970. The runaway greenhouse and the accumulation of CO_2 in the Venus atmosphere. *Nature* **226,** 1037–1039.

ROOD, R. T., AND J. S. TREFIL 1981. *Are We Alone? The Possibility of Extraterrestrial Civilizations.* Scribner, New York.

SCHATTEN, K. H., AND A. S. ENDAL 1982. The faint young sun–climate paradox: Volcanic influences. *Geophys. Res. Lett.* **9,** 1309–1311.

SCHNEIDER, S. H., AND S. L. THOMPSON 1980. Cosmic conclusions from climatic models: Can they be justified? *Icarus* **41,** 456–469.

SCHWARTZMAN, D., AND T. VOLK 1989. Biotic enhancement of weathering and the habitability of Earth. *Nature* **340,** 457–460.

SELLERS, W. D. 1969. A climate model based on the energy balance of the Earth–atmosphere system. *J. Appl. Meteorol.* **8,** 392–400.

SHKLOVSKII, I. S., AND C. SAGAN 1966. *Intelligent Life in the Universe.* Holden–Day, San Francisco.

SODERBLOM, D., AND D. LATHAM 1991. SETI microwave observing project: Target selection strategy. SETI IWG No. 2.

SOLOMON, S. C., AND J. W. HEAD 1991. Fundamental issues in the geology and geophysics of Venus. *Science* **252,** 252–260.

SMITH, B. A., AND R. J. TERRILE 1984. A circumstellar disk around β Pictoris. *Science* **226,** 1421–1424.

SUSSMAN, G. J., AND J. WISDOM 1992. Chaotic evolution of the solar system. *Science* **257,** 56–62.

UREY, H. C. 1952. *The Planets: Their Origin and Development.* Yale Univ. Press, New Haven.

VUKALOVICH, M. P., AND V. V. ALTUNIN 1968. *Thermophysical Properties of Carbon Dioxide.* Collet's, London. [translated from Russian]

WALKER, J. C. G. 1977. *Evolution of the Atmosphere.* Macmillan, New York.

WALKER, J. C. G. 1985. Carbon dioxide on the early Earth. *Origins Life* **16,** 117–127.

WALKER, J. C. G. 1991. Feedback processes in the biogeochemical cycles of carbon. In *Scientists on Gaia* (S. H. Schneider and P. J. Boston, Eds.), pp. 183–190. MIT Press, Cambridge, MA.

WALKER, J. C. G., P. B. HAYS, AND J. F. KASTING 1981. A negative feedback mechanism for the long-term stabilization of Earth's surface temperature. *J. Geophys. Res.* **86,** 9776–9782.

WETHERILL, G. W. 1986. Accumulation of the terrestrial planets and implications concerning lunar origin. In *Origin of the Moon* (W. K. Hartmann, R. J. Phillips, G. J. Taylor, Eds.), pp. 519–550. Lunar and Planetary Inst., Houston.

WETHERILL, G. W. 1991. Occurrence of Earth-like bodies in planetary systems. *Science* **253,** 535–538.

WHITMIRE, D. P., J. J. MATESE, AND L. J. TOMLEY 1988. A brown dwarf companion as an explanation of the asymmetry in the Beta Pictoris disk. *Astron. Astrophys.* **203,** L13–L15.

WHITMIRE, D. P., R. T. REYNOLDS, AND J. F. KASTING 1991. Habitable zones for Earth-like planets around main sequence stars. In *Bioastronomy: The Search for Extraterrestrial Life* (J. Heidmann and M. J. Klein, Eds.), pp. 173–178. Springer-Verlag, Berlin.

WOLERY, T. J., AND N. S. SLEEP 1976. Hydrothermal circulation and geochemical flux at midocean ridges. *J. Geol.* **84,** 249–275.

WOOLLEY, H. W. 1954. *J. Res. Natl. Bur. Stand.* **52,** 289.